GA-A20796

HIGH-TEMPERATURE CERAMIC SUPERCONDUCTORS

FOR PERIOD
OCTOBER 1, 1990 TO SEPTEMBER 30, 1991

THIRD ANNUAL REPORT
FINAL TECHNICAL REPORT

Prepared for
OFFICE OF NAVAL RESEARCH
800 NORTH QUINCY STREET
ARLINGTON, VIRGINIA 22217-5000

DARPA/ONR CONTRACT N00014-88-C-0714

APPROVED FOR PUBLIC RELEASE

Prepared by
K.S. MAZDIYASNI, PROGRAM MANAGER
F.C. Montgomery, K.C. Chen,
S.S. Pak, D.M. Duggan, L. Paulius (UCSD)
M.B.Maple, (UCSD) and P.K. Tsai (UCSD)

APPROVED BY: T. D. Gulden
T. D. Gulden
Director, Defense Materials

GENERAL ATOMICS PROJECT 3850

GENERAL ATOMICS

SECURITY CLASSIFICATION OF THIS PAGE

REPORT DOCUMENTATION PAGE

Form Approved
OMB No. 0704-0188

1a. REPORT SECURITY CLASSIFICATION: Unclassified	1b. RESTRICTIVE MARKINGS
2a. SECURITY CLASSIFICATION AUTHORITY	3. DISTRIBUTION/AVAILABILITY OF REPORT
2b. DECLASSIFICATION/DOWNGRADING SCHEDULE	Unlimited
4. PERFORMING ORGANIZATION REPORT NUMBER(S): Project 3850 GA-A20796	5. MONITORING ORGANIZATION REPORT NUMBER(S)
6a. NAME OF PERFORMING ORGANIZATION: General Atomics; 6b. OFFICE SYMBOL (If applicable)	7a. NAME OF MONITORING ORGANIZATION: Office of Naval Research
6c. ADDRESS (City, State, and ZIP Code): P.O. Box 85608, San Diego, CA 92121	7b. ADDRESS (City, State, and ZIP Code): 800 North Quincy Street, Arlington, VA 22217
8a. NAME OF FUNDING/SPONSORING ORGANIZATION: Defense Advanced Research Agency; 8b. OFFICE SYMBOL (If applicable): DARPA	9. PROCUREMENT INSTRUMENT IDENTIFICATION NUMBER: N00014-88-C-0714
8c. ADDRESS (City, State, and ZIP Code): 1400 Wilson Blvd., Arlington, VA 22209	10. SOURCE OF FUNDING NUMBERS: PROGRAM ELEMENT NO. / PROJECT NO. / TASK NO. / WORK UNIT ACCESSION NO.

11. TITLE (Include Security Classification): High Temperature Ceramic Superconductors

12. PERSONAL AUTHOR(S): K.S. Mazdiyasni

13a. TYPE OF REPORT	13b. TIME COVERED	14. DATE OF REPORT (Year, Month, Day)	15. PAGE COUNT
Annual Report	FROM 10/1/90 TO 9/30/91	December 15, 1991	97

16. SUPPLEMENTARY NOTATION

17. COSATI CODES		
FIELD	GROUP	SUB-GROUP

18. SUBJECT TERMS (Continue on reverse if necessary and identify by block number)
Sol-Gel; Melt Texturing; Precursor Compounds; Fiber; Electromagnetic properties; Processing; Flux Creep; Microstructures

19. ABSTRACT (Continue on reverse if necessary and identify by block number)

The principle goals of this program were (1) to demonstrate fabrication of high-temperature ceramic superconductors via sol-gel method that can operate at or above 90K with appropriate current density, J_c, in forms useful for application in resonant cavities, magnets, motors, sensors, computers, and other devices; and (2) to fabricate and demonstrate selected components made of these materials, including microwave cavities and magnetic shields. Chemical pathways for synthesis of 123 identified, process parameters window for sol-gel derived 123 fibers established, continuous flexible fibers 15-200 μm in diameter produced fibers with T_c ~92.5 K, ΔT=1.5 K, $J_c = 2 \times 10^3$ A/cm^2 at 77K, 0 field; 4×10^3 at 57K, 100 Oe produced. Melt textured fibers had $J_c = 2 \times 10^3$ A/cm^2 at 77K in 1.2 Tesla field. praseodymium addition to 123 showed potential improvement in flux pinning of high T_c superconductor.

20. DISTRIBUTION/AVAILABILITY OF ABSTRACT	21. ABSTRACT SECURITY CLASSIFICATION
☒ UNCLASSIFIED/UNLIMITED ☐ SAME AS RPT. ☐ DTIC USERS	
22a. NAME OF RESPONSIBLE INDIVIDUAL: Dr. Wallace Ar Smith	22b. TELEPHONE (Include Area Code): 202-696-0284; 22c. OFFICE SYMBOL: ONR

DD Form 1473, JUN 86 — Previous editions are obsolete. — SECURITY CLASSIFICATION OF THIS PAGE

FOREWORD

This report summarizes mostly experimental work conducted during the third and final year, October 1, 1990 to September 30, 1991, of DARPA/ONR Contract N00014-88-C-0714, High Temperature Ceramic Superconductors. Dr. Frank W. Patten is the DARPA program manager and Dr. Wallace Arden Smith, Materials Division, Department of the Navy, ONR, is the Navy project scientist.

Also included as part of this summary technical report is an appendix which covers more detailed experimental aspects of the work performed during the last year of the research program.

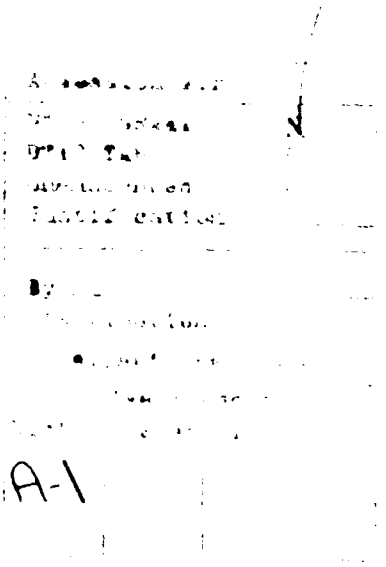

TABLE OF CONTENTS

1. INTRODUCTION

Some encouraging work on the production of bulk conductor forms, such as wires, cables, and tapes is being reported. This work is mainly driven by the realization that usable magnets and solenoids made from high T_c materials will be of major technological and economic importance. Their impact will be far reaching in both military and civilian applications.

Still the overriding issue in bulk superconducting materials today is, that of materials synthesis and processing. In general, the HTS materials are made in bulk form by a number of approaches. The simplest is, of course, milling together of binary oxides and/or carbonates. This method can be highly effective in making laboratory samples, but it lacks control of particle morphology and requires long milling times to achieve homogeneity and small particle size. Chemical methods of preparation include coprecipatation methods (Ref. 1-2) and sol-gel (Refs. 1, 3 and 4) processes. While in principle these methods appear to be more advantageous than milling, in practice their full potential has yet to be realized. Precursor powders have also been successfully produced by dry roasting nitrate solutions. Freeze drying (Ref. 5) of the solution produces uniform fine powders. Related to these processes are the use of the aerosol flow reactor (Ref. 6) and the total combustion burner (Ref. 7), where aerosol droplets are formed from suitable inorganic salt solutions. Regardless of powder precursor source, the bulk forms are made only by high temperature processing, i.e., temperatures of 900° to 1000°C. This makes reactions with container materials difficult to control, and purity of the HTS is difficult to achieve. In addition to processing difficulties, the oxygen content is difficult to control, especially in dense bodies, and very temperature dependent, reproducible samples of good quality are difficult to ensure.

The second critical issue is to understand processing/microstructure/properties relationships and the underlying physical properties, particularly J_c and flux pinning issues. This task will not be easy because in processing ceramic materials, in general, the goal is to obtain a uniform fine grained material in order to obtain the best mechanical properties. This is of particular importance in ceramic materials that exhibit large anisotropy in thermal expansion, where studies have shown that microcracking occurs when grain size in a randomly oriented structure exceeds a critical value determined by the material parameters (Ref. 8), as may be expected considering the large anisotropy in the thermal expansion of yttrium barium cuprate, especially at the tetragonal to orthorhombic transition. The phase instability not only results in mechanical property degradation; but also the microcracks act to limit the electrical contact between grains, which contributed to the weak link behavior in the bulk superconducting properties of these materials. A recent study (Ref. 9) has found a critical grain size of the order of 1 micron for randomly oriented 123 compound. It is therefore apparent that in order to achieve high values of J_c in bulk material, dense material with grain size less than this must be produced. Due to the anisotropy in the superconducting properties of these materials, it is also necessary to produce grain-aligned material in order to obtain the maximum J_c. It may be expected that the production of aligned material will relax the grain size requirement somewhat, but if alignment is less than perfect, effects of anisotropy in thermal expansion will still be evident.

In view of these observations on processing, it is evident that beside grain boundaries, which are the dominant cause of low J_c in 123 polycrystalline material, a number of other factors may also contribute to decreasing the attainable critical current densities. The relative importance of issues such as grain-

boundary phase, carbonate retention, environmental stability, micro-and macrocracking phenomena, etc., remains to be addressed. Thus, it is clear that assessing the influence of any one factor requires careful control of the others and that attainment of the highest J_c may require simultaneous optimization of several of these factors.

For most applications, however, two fundamental hurdles must be overcome to produce long length HTS conductors that enable significant improvements in systems. These hurdles are (1) weak intergrain links and (2) weak flux pinning.

Intergrain links are the electrical contacts between individual grains of the HTS materials, and these contacts are generally resistive as a result of crystal misalignment and contamination at grain boundaries aggravated by the very short coherence lengths in these materials. Weak intergrain links result in low current limits and sensitivity to magnetic fields.

As the intergrain links are improved, wire will become feasible with moderate-to-good properties. In particular, it is likely that wire with about 10 kA/cm^2 at a field of >1 Tesla and a temperature of 77K should be achievable in unlimited lengths (research materials are now approaching this performance).

Once the weak intergrain link problem is resolved, flux pinning will be the major hurdle for improving bulk conductors. Flux pinning is essential for high field applications and especially for ac or time-varying applications. The magnetic flux lines are pinned, or held in place, by microscopic regions of non-superconducting material. Arranging such pinning centers in the HTS material without destroying its overall superconductivity is a major challenge.

If strong flux pinning can be arranged, in addition to good grain-to-grain contacts, then wire with superior electromagnetic properties should result, exhibiting as much as 100 kA/cm^2 in fields of several Tesla at temperatures up to 77K.

Three promising techniques for improved flux pinning have already been demonstrated. One involves neutron irradiation of the bulk material, creating isolated defects that pin flux lines and result in higher field tolerance within a grain. In a related development, proton beams were used to create non-superconducting regions deep within HTS grains, similarly resulting in flux pinning sites. The third approach which is favored at GA, uses non-reactive second phase and/or nano size particulate "precipitate" to act as pinning sites. Even at the present early stage in the development of these approaches, the material properties available would be sufficient for select applications if they were incorporated in a practical wire or other conductor configuration.

1.2 PROGRAM OBJECTIVES

The original principle goals of this program were (1) to demonstrate fabrication of high-temperature ceramic superconductors via a sol-gel method that can operate at or above 90K with appropriate current density, J_c, in forms useful for application in resonant cavities, magnets, motors, sensors, computers, and other devices; and (2) to fabricate and demonstrate selected components made of these materials, including microwave cavities and magnetic shields.

The General Atomics (GA) approach is to develop the sol-gel technology processing of high-temperature ceramic superconductors to make sol-gel a viable process for fabricating high T_c (90 K) superconductors in forms useful for applications. The nature of

sol-gel processing makes it inherently amenable to fabricating the thin films and fibers that are needed for many applications. In addition, the relatively low temperature characteristics of sol-gel processing make it advantageous for many applications in which the superconducting materials must be applied to heat sensitive substrates.

The scope of the effort includes the following:

- Synthesis of sol precursors
- Optimization of sol-gel processed materials, including purity, homogeneity, stoichiometry, sintering temperatures, grain size and orientation, and dopants for grain boundary and flux pinning and for control of mechanical properties.
- Fabrication of forms, including powders, thin and thick films, and fibers.
- Evaluation of environmental stability, physical, mechanical, electrical, and magnetic properties.
- Fabrication and testing of a model component.

1.2.1 PROJECT OUTLINE

This program has been divided into six tasks: (1) metal alkoxide synthesis and processing, (2) microstructural evaluation and property measurement, (3) electrical and magnetic property measurement, (4) superconductor ceramic processing, (5) component fabrication and demonstration, and (6) reporting.

Task 1 is to synthesize a homogeneous metal alkoxide, $M(OR)_n$, where n is the valence of metal, M, and R is an organic group, solution that contains all the constituent elements which can be easily made to powders, thin film, or drawn into fiber form. Ideally, this solution should possess precise

stoichiometry, adequate stability, polymerizability, adherence, and spinnability. Also, the polymeric materials formed from this solution should be thermosetting, be able to be dissolved in organic solvents, and contain as little as possible low-temperature pyrolyzable organics with high char yield.

Task 2 is to study the microstructure as a function of processing parameters. The study includes: density, pore size and pore size distribution, phase identification, chemical composition and purity, environmental stability, effects of heat treatment, residual strain, seeding, annealing in magnetic fields, and epitaxy on grain growth and orientation.

Task 3 is to study the electrical and magnetic properties of the $YBa_2Cu_3O_{7-x}$ (123) high T_c ceramic superconductors. It will include both the ac electrical resistance (R_{ac}) and the magnetic susceptibility (X_{ac}) magnetic properties.

The dc current versus voltage curve will be measured at liquid nitrogen temperatures for all promising superconducting materials and a value for J_c (77 K) determined. For the samples with the highest values of J_c (77 K), critical currents will be measured as a function of magnetic fields of up to 8 Tesla at temperatures between 1.4 K and near the superconducting transition temperature T_c. These data will be collected in liquid He or flowing He using a Janis Supervaritemp dewar equipped with an 8 Tesla superconducting magnet. As required, Hall effect measurements can be performed in this apparatus to determine the type and density of the current carriers. Both X_{ac} and R_{ac} at pressures up to 20 kbar, can be used in this dewar to measure the superconducting and magnetic properties of samples at high pressures, at high magnetic fields, and at temperatures from 1.4 to 300 K.

As a subcontractor to GA, the Superconductivity and Magnetism group, under the direction of Professor M. Brian Maple, at the University of California, San Diego (UCSD), has performed the electromagnetic characterization of high-temperature superconducting oxide compounds, which are fabricated at GA. UCSD personnel have and will continue to measure the superconducting and magnetic properties by means of measurements of the upper critical magnetic field, critical current density inferred from both direct and magnetization measurements, magnetic susceptibility, Meissner effect and specific heat.

Task 4 is an investigation of superconductor ceramic processing. Most of the important applications of superconductors require material in the form of fiber or films. Magnets, conductors, motors and generators are examples of applications employing fiber; while detectors, microwave cavities, and microcircuitry require superconducting material in the form of films. The sol-gel process is ideally suited to producing materials in these forms; in fact, it is used commercially to produce anti-reflection and mirror coatings and to produce continuous ceramic fibers for structural reinforcement in composite materials and for thermal insulation.

Originally, Task 5 was to demonstrate component fabrication. GA under the original SOW had to design and build a high Q, high T_c superconducting cavity using its unique sol-gel coating processing capabilities. This task would have proceeded after some initial coating tests verified dc superconductivity and questions of adhesiveness, surface preparation, and processing procedure are answered. As the fabrication process and the materials quality were improved throughout the three-year program, two additional cavities would have been constructed and tested. Coupling would have been through a waveguide inductive iris into an end wall with a logarithmic decrement technique of Q

measurement were considered most appropriate for the high Q anticipated. An X-band (10 GHz) frequency choice allows for convenient dimensions of 4.3 cm diameter by 2.8 cm height. However, DARPA/ONR recent recommendation to GA was to curtail the work on the cavity and concentrate on improving the quality and transport properties of solution condensed films.

2. SUMMARY OF ACCOMPLISHMENTS*

In the following section, a brief narrative description of the major advances that have been accomplished during the third year under the subject contract are presented.

2.1 Ceramic Superconductor Fiber Processing

1. Fabricated 20-18 microns diameter flexible sol-gel Y123 fibers
2. Improved fiber morphology (eliminated waviness)
3. Obtained uniform small grain size in spun fibers.
4. Achieved T_c, 50% ( ) = 87-92K and T(90%-10%)=1.5-2K
5. Measured J_c of 3500 A/cm^2 (77K) and 1x10^4 A/cm^2 (50K) at 0 magnetic field.

2.2 Melt texturing of sol-gel derived Y123 fibers

1. Designed and built furnace for melt texturing
2. Melt textured short length, 3 cm x 200 microns diameter fibers
3. Increased J_c to 2 x 10^3 A/cm^2 (77K) with magnetic field strength of 1.2 Tesla

*Other accomplishments under this program were reported in annual reports #GA-A19800 and GA-A20346

3. PUBLICATIONS AND PRESENTATIONS

3.1 PUBLICATIONS

1. Chen, K.C., and K.S. Mazdiyasni, "High T_c Superconductor Fibers from Metallo-Organic Precursors," MRS Proceeding, Vol. 69, pp 1213-1216 (1990).
2. Chen, K.C., A.Y. Chen, and K.S. Mazdiyasni, "Metallo-Organics Derived Tractable Resins for YBCO Superconducting Fiber Fabrication," published in MRS Proceeding Better Ceramics Through Chemistry, Vol. 180, pp 913-916 (1990).
3. Stephens, R.B., "Flux Bundle Interactions", Jour. of Mat. Res. Society, Vol. 5, No. 12, (1990).
4. L.M. Paulius, P.K. Tsai, J.J. Neumier, M.B. Maple, K.C. Chen and K.S. Mazdiyasni, "Flux Pinning in Y_{1-x} Pr_x Ba_2 Cu_3 $O_{7-\delta}$ High T_c, Superconductor", Applied Phys. Letter, 58 (16) 22 April 1991.
5. S.S. Pak, F. Montgomery, D.M. Duggan, K.C. Chen, K.S. Mazdiyasni, P.K. Tsai, L.M. Paulius and M.B. Maple "Solution Condensed $YBa_2Cu_3O_{7-x}$ Superconductor Thin Films from Thermosetting Metal-Organic Precursors" to be published in the J. Am. Ceram. Soc. (1992).

3.2 PRESENTATIONS

1. Sung, S.P. and K.S. Mazdiyasni, "Sol-Gel Synthesis and Characterizations of Submicron High T_c Ceramic Superconducting Powders," Third International Conference on Ceramic Powder Processing Science, San Diego, CA, February 4-7, 1990.

2. Chen, K.C., A.Y. Chen, and K.S. Mazdiyasni,"Sol-Gel Derived Soluble Resin for Y-Ba-Cu-0 Superconducting Fiber Fabrication" presented at Materials Research Society 1990 Spring Meeting, Symposium A: Better Ceramics Through Chemistry IV, San Francisco, CA, April 16-21, 1990.

3. Chen, K.C., A.Y. Chen and K.S. Mazdiyasni, "Synthesis and Characterization of Tractable Resin for YBCO Superconducting Fibers Fabrication," presented at the 92th Annual Meting of American Ceramic Society, Dallas, Texas, April 24, 1990.

4. Stephens, R.B., "Flux Bundle Interactions," presented at MRS Spring Meeting, Anaheim, CA 1990.

3.3 PATENTS

1. Chen, K.C. and K.S. Mazdiyasni, "Method for Preparing Rare Earth-Barium-Cuprate Preceramic Resins and Superconductive Materials Prepared Therefrom," U.S. Patent Application No. 441,955, allowed.

2. Chen, K.C. and K.S. Mazdiyasni, "Method for In-Situ Prevention of Stable Barium Carbonate Formation in High T_c Ceramic Superconductors." U.S. Patent Application Sa1,564, allowed.

3. Chen, K.C. and K.S. Mazdiyasni, "Method for In-Situ Prevention of Stable Barium Carbonate Formation in High T_c Ceramic Superconductor", U.S. Patent Application 591,440, allowed.

REFERENCES

1. Barboux, P., J.M. Tarascon, L.H. Green, G.W. Hull, and B.G. Bagley, J. Appl. Phys., 63, 2725 (1988).

2. Dun, B.C., T. Chu, L.W. Zhow, J.R. Copper, and G. Gruner, Adv. Ceram. Mater., Suppl. 2, 343 (1987).

3. Kordas, G., K. Wu, U.S. Brahme, T.A. Friedman, an D.M. Ginsberg, Mater. Lett., 5, 417 (1987).

4. Accibal, M.A., J.W. Draxton, A.H. Gabor, W.L. Gladfelter, B.A. Hassler, and M.L. Mecartney, "Better Ceramics Through Chemistry III," edited by C.J. Brinker, D.E. clark and D.R. Ulrick (MRS Proc. Vol. 121).

5. Johnson, S.M., M.I. Gusman, D.J. Rowcliff, T.H. Gegalle and J.Z. Sun, Adv. Ceram. Mater., 2, 337 (1987).

6. Kodas, T.T., E.M. ENgler, V.Y.Lee, R. Jacowitz, T.H. Baum, K. Roche, S.S.P. Parking, W.S. Young, S. Hughes, J. Kleder and W. Auser, Appl. Phys. Lett., 52, 1622 (1987).

7. Merkle, B.D., R.N. Kniseley, F.A. Schmidt, and I.E. Anderson, J. Mater. Sc. and Eng. (to be published).

8. Dole, S.L., O. Hunter, Jr., F.W. Calderwood and D.J. Bray, J. Am. Ceram. Soc., 61, 486 (1978).

9. Shaw, T.M., S.L. Shinde, D. Ramos, R.F, Cook, P.R. Duncombe and C. Kroll, J. Mat. Research, Vol. 4, NO. 2, 248-256 (1989).

APPENDIX A CERAMIC SUPERCONDUCTOR FIBER PROCESSING

A-1. FABRICATION OF 20 MICRON DIAMETER Y123 FIBERS

In order to improve the flexibility of superconducting fibers for subsequent melt texturing, the diameter of the final heat-treated fiber was targeted to be 20 micron (down from usual 100 micron described in the previous annual reports). To account for the approximately 50-60% shrinkage during heat treatment of the precursor fibers, and assume fiber is to be made by simple extrusion without down-drawing, the opening of the spinneret (die) was set at 50 micron. Due to the precision and smoothness requirements, the die was ordered from Fitech (Italy) (Fig. 1). It is possible to further reduce the diameter of the fiber to 10 micron by stretch-spinning, but the control of processing parameters or handling of the fiber become much more difficult. However, as the fiber diameter is reduced from 100 micron to 20 micron, some processing parameters had to be modified.

A-1.1 MIXING AND FILTERING

Mixing of the "resin," developed and reported previously, with the binary (polar and non-polar) solvents should be more uniform than previously required since slight inhomogeneity in the resin mass greatly influences the fiber extrusion pressure, or even blocking the opening of the die. It also affects the final fiber mechanical and electrical properties. To improve the uniformity of the resin mass, the resin powder was ground and

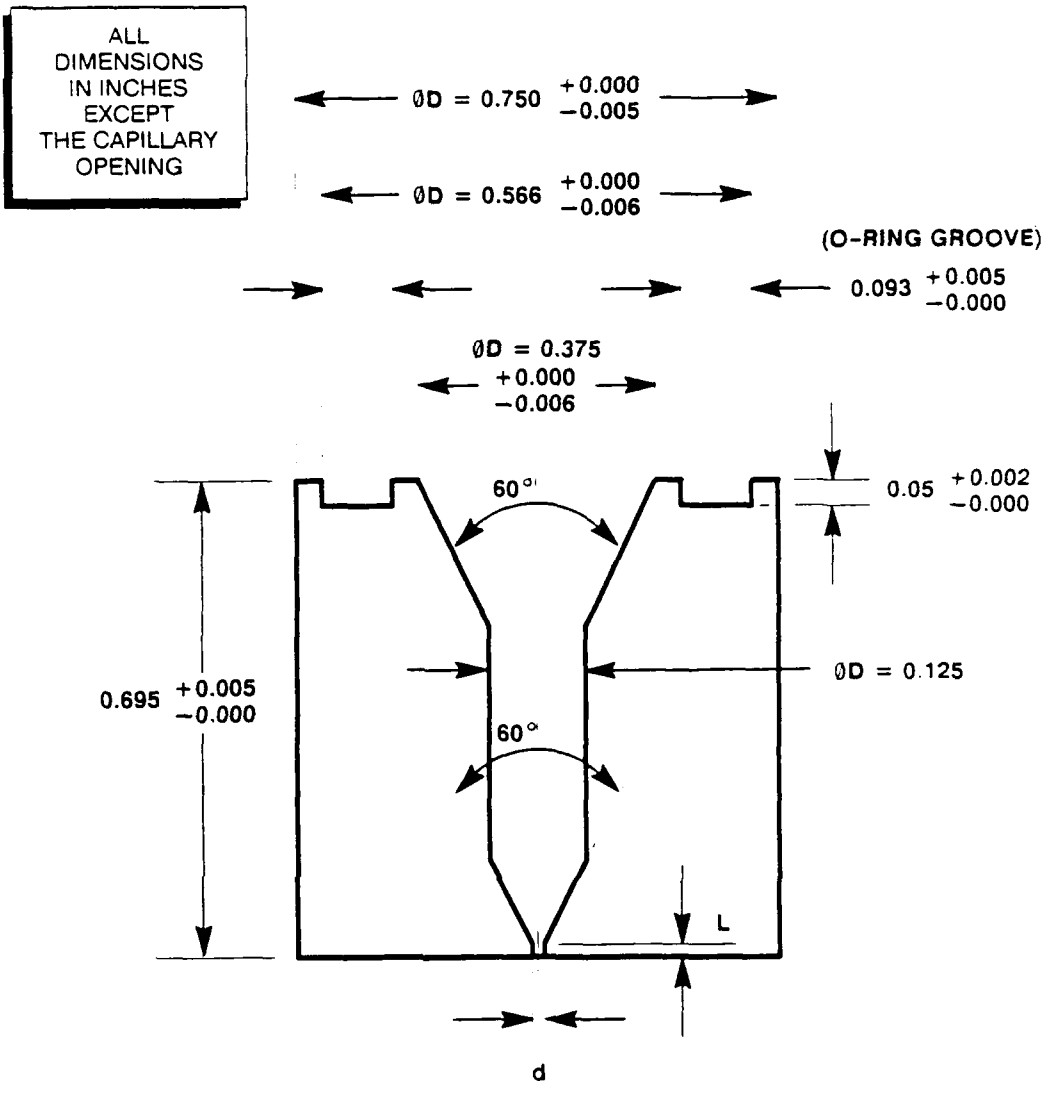

INSTRUCTIONS

- **ROUND HOLE DIAMETER d = 0.05 mm L/D = 0.07 – 1**
- **TOLERANCE AS STANDARD FOR WET AND DRY SPINNING MIRROR FINISH AT THE CAPILLARY OPENING: 0.02 – 0.05 μ**
- **MATERIAL: STAINLESS STEEL**
- **O-RING FACE GROOVE FOR PARKER NO. 2-013 O-RING**

O.D. = 0.566 +0.000 −0.006

DEPTH = 0.050 +0.002 −0.000

WIDTH = 0.093 +0.005 −0.000

K-181(5)(I-01)
8-9-91

Fig.1. The die used for extrusion of 50 μm precursor fiber.

sieved through a 50 microns sieve so no particles larger than 50 micron in size could pass through.

A-1.2 EXTRUSION PRESSURE

The pressure required for a smooth continuous spinning line was studied by using an Instron machine. With simple extrusion and no down-drawing, it was found that when the pressure was too high (300-400 lb load, 3600 psi), a melt fracture always occurred resulting in a wavy and kinky fiber. Often, this instability led to entanglement in the fiber line. Kinks and entanglement still happened quite frequently at slightly lower pressure (>1620 psi). A stable fiber spinning line was maintained at 750 to 1350 psi (80-150 lb load). For initial pressure within this range, stable fiber line was sustained for approximately 20-40 min while the pressure gradually decreased. Below 70 psi, no fiber could be extruded. However, pressure needed to maintain the stable fiber line increased as the piston moved down due to the greater friction between the piston and the die wall. Therefore, a constant downward movement of the piston was needed. The downward speed required to maintain this pressure is in the range of 0.002 in./min or below but, due to the contractual funding constraints, this parameter was not precisely determined.

Thus, a compromise had to be made between the extrusion pressure and the output rate of the fiber. Toward the upper pressure limit of the stable fiber line, output rate greater than approximately 1.5 cm/sec can be achieved but the drawback seems to be the fiber line stability. The extruded 50 microns precursor fibers

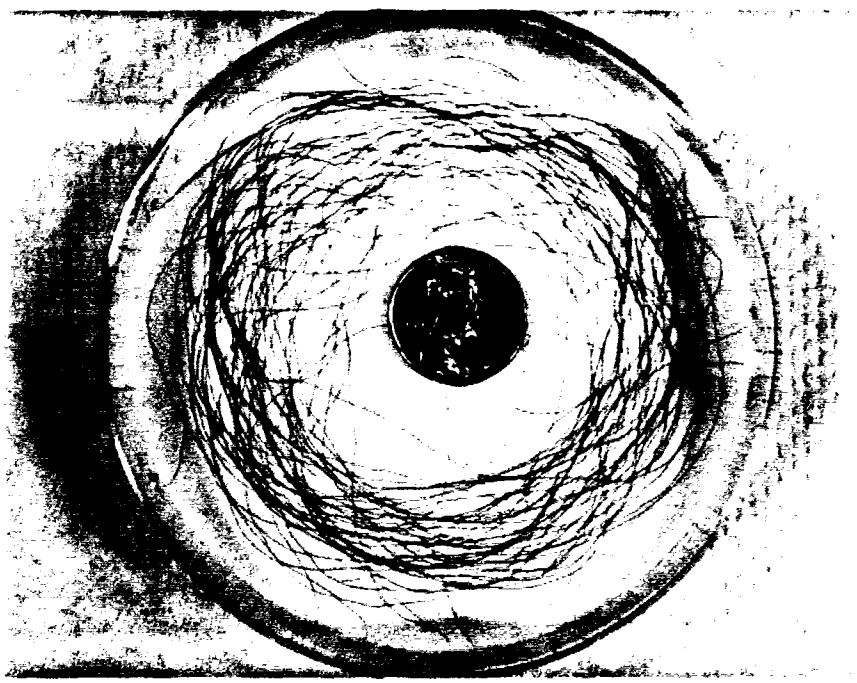

Figure 2. The extruded 50 micron precursor fibers.

conditions of 50 microns precursor fiber was not established, the simultaneous down stretching was not performed. With a simultaneous down-drawing, a final sintered fiber of 10 microns diameter could be made possible.

A-1.2.1 REMOVING WAVINESS (straighten process) OF THE FIBER

It was discovered that for the precursor fibers to have uniform diameter with minimum waviness, a short time annealing at 175-180°C was required to remove this waviness and straighten the fiber. DSC study indicated a possible irreversible relaxation process occurring in the temperature range of 75-175°C. A reversible thermal effect also occurred below 63°C. Figure 3(a), shows the DSC trace of precursor fibers in nitrogen atmosphere and Fig. 3(b) is the re-run trace after cooling. The very broad endothermic peak disappeared by the first heating but the larger endothermal peak remained. Even with the 180°C straighten process, the waviness occurred if heating rate greater than 0.5°C/min was maintained. The occurrence of the waviness during the high heating rate treatment schedule was thought to be due to overheating. Overheating caused very slight melting in the interior of the fiber and redistribution of the liquid phase.

In summary, some modifications in the extrusion die and determination of processing parameters were needed in order to fabricate 20 microns superconducting fibers.

A-2 PRELIMINARY TESTING OF THE 20 MICRONS SUPERCONDUCTING FIBERS

Straight 18-20 microns diameter superconducting fibers were obtained after heat treatment. Some fibers exhibit

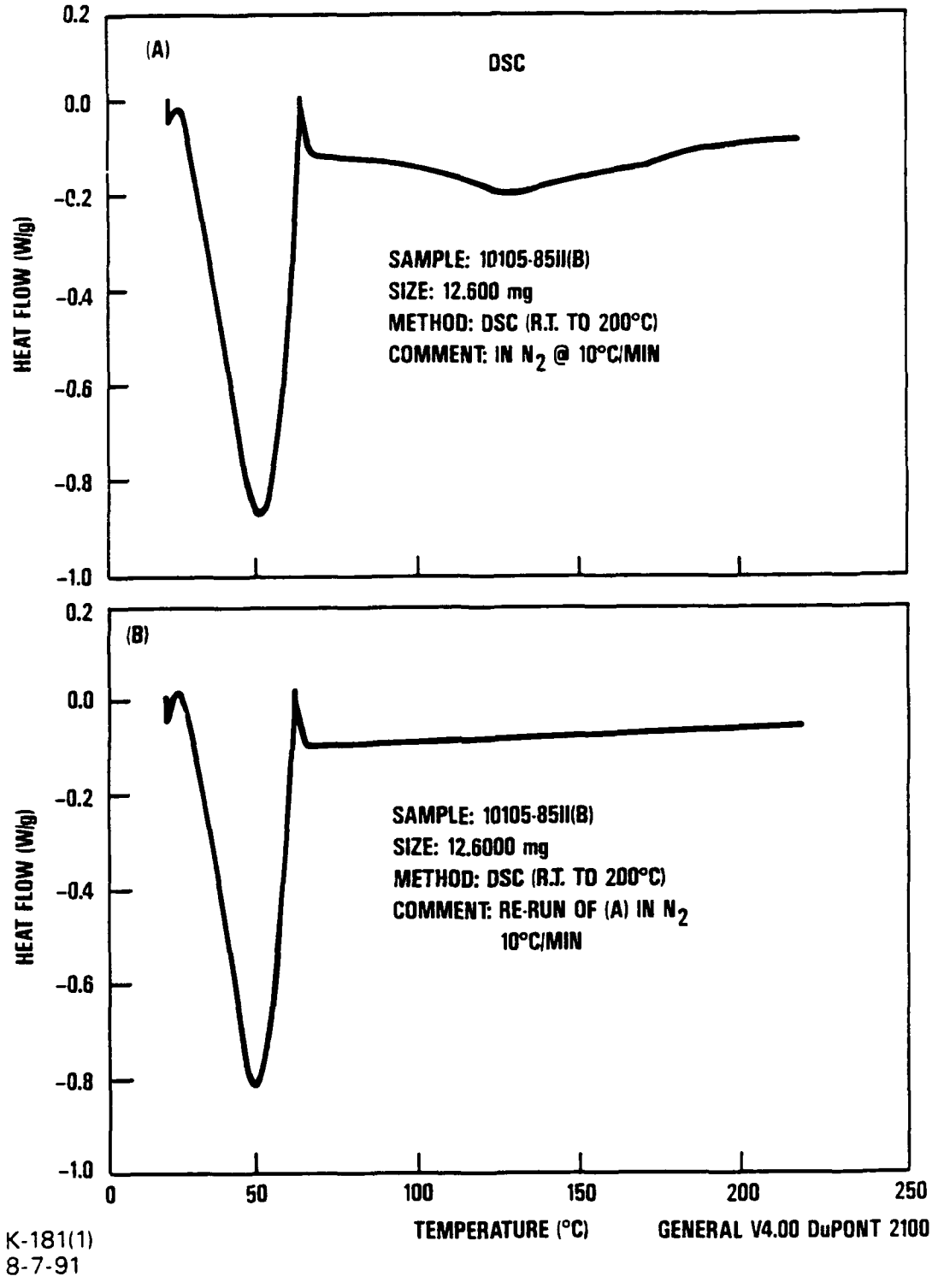

Fig. 3. DSC curves of precursor fibers showing an irreversible endothermal peak from 75-175°C and a reversible peak at 50°C; (a) first run (b) re-run of the same sample.

excellent flexibility but others did not. A radius of curvature as small as 2-3 cm was achieved. However, in these flexible straight fibers some microstructure defects, such as small surface cracks and large pores, still exist (Fig. 4). The microstructure defects inevitably reduces the tensile strength of the fiber. By removing these defects, fibers will be much stronger. The handling and applying current contacts and silver lead wires to these 20 microns fibers pose some challenge. Some micro-tools are required to routinely handle these fibers for testing.

The electrical properties of these 18-20 microns superconducting fibers were measured. The T_c in the temperature range of 92-89K were attained. This depends on heat treatment schedule and resin batches. Occasionally, small tails occurred in the resistance versus temperature curve which lowers the T_c (R=0) to about 75-80K. A maximum J_c value of $1X10^4$ A/cm^2 (50K, ambient field) has been observed in 18 micron diameter fibers where I_c is ~16-19mA. The J_c values varied with heat treatment and somewhat scattered. This may be due to the microstructure defects described above.

A-3 MELT TEXTURING OF SOL-GEL DERIVED FIBERS

A-3.1 INTRODUCTION

Melt-texturing has proven to be an effective technique in improving the current carrying capacity of polycrystalline $REBa_2Cu_3O_{7-x}$, [1-5] where RE is a rare earth element. Despite the remarkable success, the technique used has been slow and cumbersome due, in part, to the sluggish crystallization kinetics of the

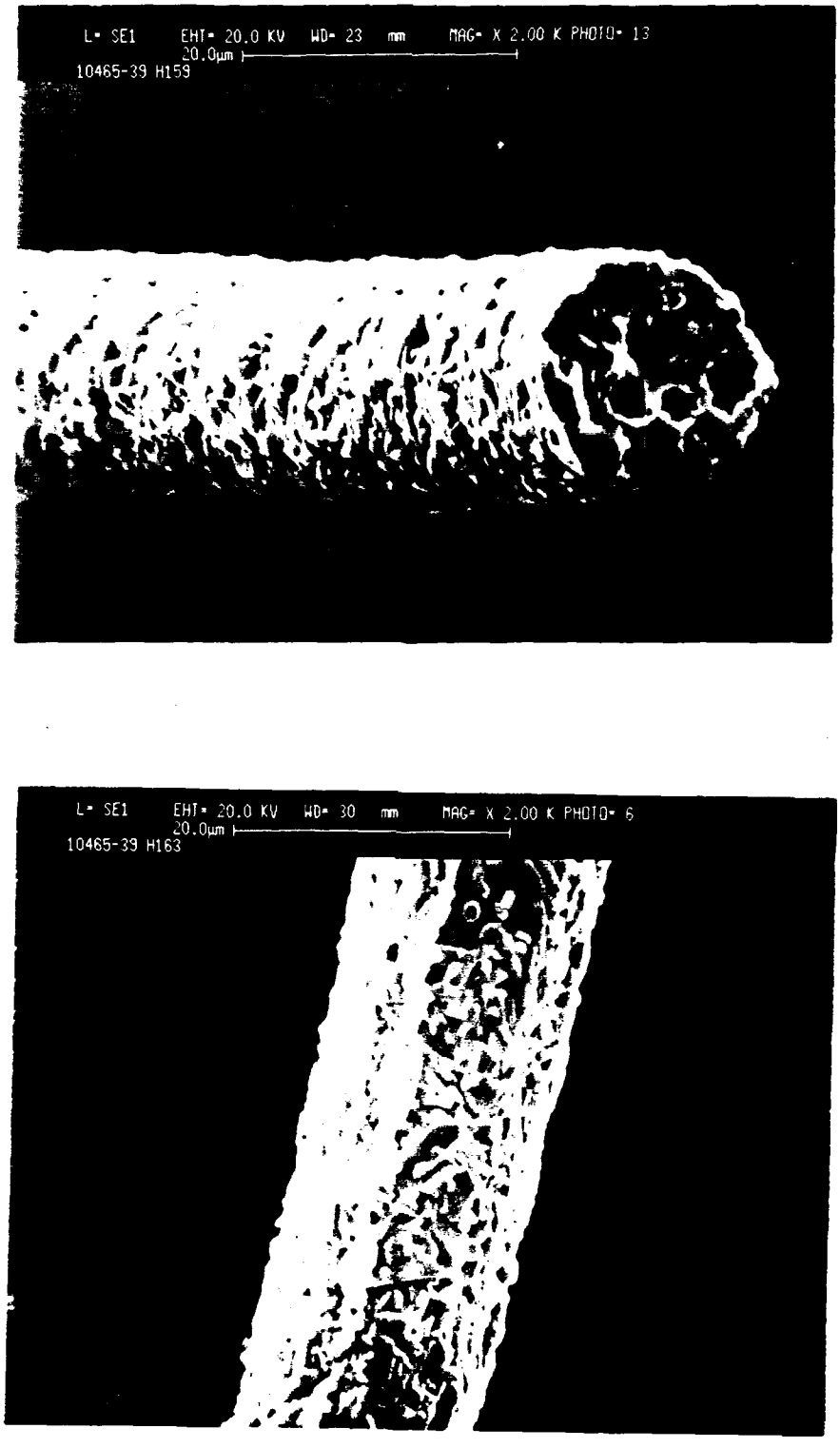

Figure 4. Some microstructral defects observed in the 20 µm superconducting fibers; (a) porosity and (b) surface crack.

superconductor. It is well established that the crystallization of $YBa_2Cu_3O_{7-x}$ from Y_2BaCuO_5 and Ba-Cu-O liquid [2] rarely ever goes to completion. Invariably, all the high quality samples reported in the literature thus far have been processed at a speed not exceeding approximately mm/hr.[7-11]. Processing speed is an extremely important economic consideration and hence must be significantly increased if high T_c superconductor fibers are to see commercialization. [12]

Numerous modified melt-texturing methods, such as the Quench-Melt-Growth, [13,14] the Melt-Powder-Melt-Growth, [15] and the Powder-Melt-Process [16] have been proposed. However, all these techniques have been developed to increase the flux pinning capability of $YBa_2Cu_3O_{7-x}$ by finely distributing Y_2BaCuO_5. Limited attempt has been made at present to increase the melt-texturing speed, while maintaining high J_c in applied magnetic field.

Under this program, at GA we have concentrated our effort to obtain a high critical current density in the fibers, while maintaining a relatively rapid pulling rate. The effects of various temperature profiles and processing speeds on fiber microstructure and Jc vs. H have been investigated. Our preliminary results on melt-texturing of sol-gel derived small diameter fiber were marginally successful. We were able to obtain samples of J_c (H=0 and T=77K) = 800 A/cm^2 using a temperature gradient of 17°C/mm near the peritectic melting point of $YBa_2Cu_3O_{7-x}$ at a processing speed of 0.4 mm/min. However, the J_c performance under an applied magnetic field was quite poor. The reason for this was mainly due to the problem arising from the positioning of the small diameter fiber in

the furnace and maintaining uniform heating during melt texturing. In our continued effort to improve the critical current density of the fibers, while maintaining a relatively rapid pulling rate, large diameter 300 μm in size fiber was used with good success.

A-3.2 EXPERIMENTAL PROCEDURE

Large diameter 300 microns sol-gel derived, stoichiometric $YBa_2Cu_3O_{7-x}$ fibers were sintered at 920°C for 2 hr in flowing O_2 prior to melt-texturing. The sintered fibers were cut to pieces that are approximately 3 cm in length. They were partially inserted in one end of a 0.4 mm I.D. alumina tube[1] whose other end was locked to a linear actuator. The fiber was secured to the tube by placing a drop of alumina glue[2] and cured at 200°C.

The fibers were melt-textured through 3 different furnaces by pulling the alumina tube at a rate between 1.04 and 0.082 mm/min. Schematic diagrams of fiber position with respect to the furnaces and their driving mechanisms are shown in Figures 5 through 7. The three furnaces were specifically designed to provide a wide range of temperature profiles, as shown in Fig. 8. The temperature in each furnace was controlled by a microprocessor[3] to minimize the fluctuation below ± 1°C. Furthermore, all the melt-texturing experiments were performed in stagnant air to minimize convection induced sample vibration.

---

[1] McDaniel Refractory Company, PA

[2] Aremco Products, Inc., NY

[3] Model CN9111, Omega, CT

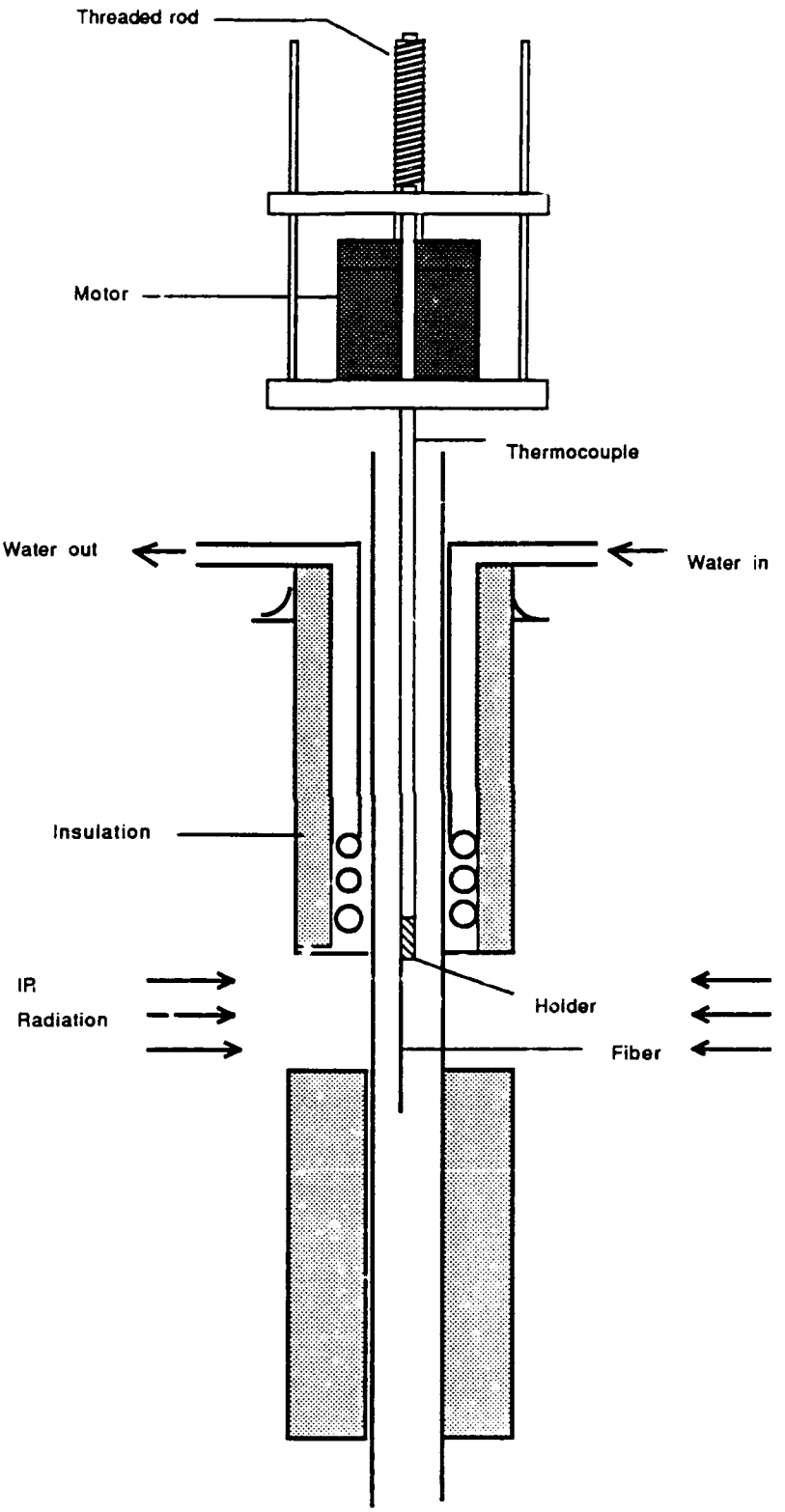

Fig. 5. Schematic diagram of the IR melt-texturing furnace. The two IR lamps are equiped with two Al concave mirrors whose focal points are at the center of the quartz tube. The zone above the hottest point is cooled by a copper tube with circulating water inside.

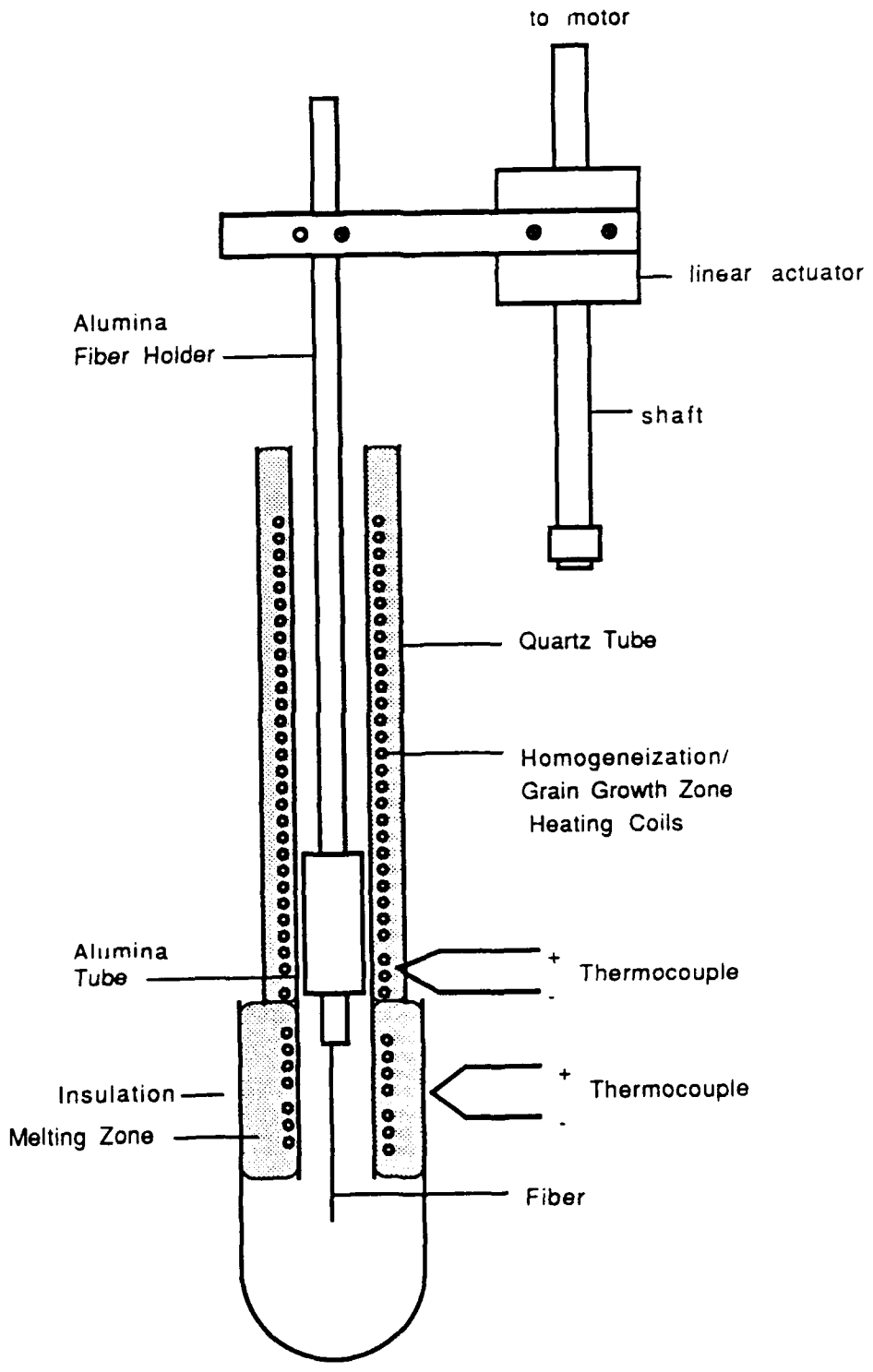

Fig. 6. Schematic diagram of the double zone furnace. Note the two heaters in series.

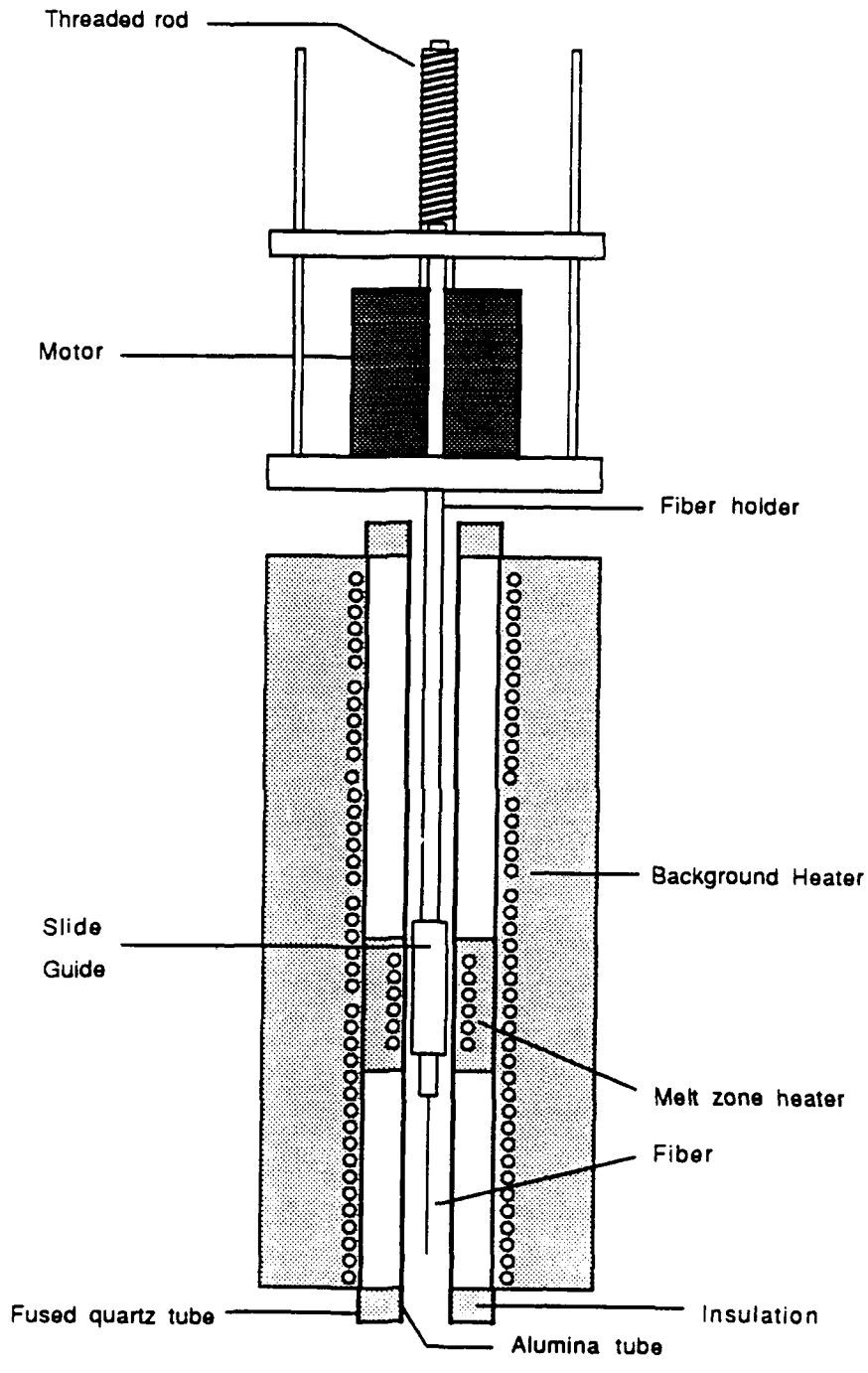

Fig. 7. A schematic diagram of the gradual cooling furnace. Note the heating insert.

After melt-texturing, the fibers were coated with a layer of fine Ag powder at 4 places along their length and heated up to 800°C at 10°C/min in flowing oxygen. After holding for 1 min, they were cooled to 500°C at 5°C/min, at which point an isothermal dwell of 24 hr was performed for full oxygenation.

The critical temperature, T_c, was measured by the standard 4 point test and the transport critical current density, J_c, by using a 0.2 μV criterion, while applying a magnetic field** up to 1.2 T at 77K.

Microstructural characterization was carried out by optical microscopy under cross polarized light and scanning electron microscopy (SEM), combined with backscattered electron imaging and energy dispersive X-ray spectroscopy (EDXS).

As stated before, because of electrostatics, it was extremely difficult to prevent 50 μm and smaller diameter fibers from sticking to the furnace inner wall. Therefore, all the melt-texturing was done on fibers with diameter grater than 200 μm.

A-4 RESULTS AND DISCUSSION

When a fiber was melt-textured through a furnace whose temperature profile was as shown in Fig. 8 (curve a), one begins to see significant grain anistropy and alignment at a pulling rate slower than 0.25 mm/min, Fig. 9. However, it can be clearly seen from the micrograph that significant porosity still remains and as the back scattered electron image, Fig. 10, and energy dispersive X-ray spectroscopy show many grain boundaries are coated with a layer of CuO. Its presence is an immediate indicator of

incomplete peritectic reaction. It is quite well established that these residual nonsuperconducting grain boundary phases act as Joshephson junctions and therefore impede high critical current density.

In order to eliminate and/or minimize the second phase from the grain boundaries, while maintaining high processing speed, an additional heater was added on top of the original heater. A schematic diagram of the furnace is shown in Fig. 6. Its temperature profile is shown by curve b in Fig. 8. The purpose of the first heater was to induce a constant, planar growth front perpendicular to the fiber axis by establishing a sharp temperature gradient near the peritectic melting point of the superconductor. And, because of the sluggish nature of crystallization, the temperature of the secondary heater was maintained just below the melting point of $YBa_2Cu_3O_{7-x}$, so that there would be ample thermally induced atomic mobility to render the crystallization of residual unreacted phases into the thermodynamically stable 123 phase. As curve b in Fig. 8 shows, the resulting temperature profile consists of a sharp temperature gradient of 17°C/mm, followed by a plateau at 965°C.

The effect of the additional heater on the microstructure is shown in Fig. 11. As the upper micrograph shows, hardly any alignment was induced with a single gradient at a pulling rate of 1 mm/min. However, the secondary heater induced significant anisotropy in grain morphology as well as their alignment, as shown by the bottom optical micrograph. Additionally, noticeable decrease in porosity is evident. Partial grain alignment and higher density are responsible for the improved J_c of the fiber, as shown in Fig. 12. Curve 49-1 represents the fiber melt-textured with just one heater, while curve 61-1 represents the fiber melt-textured with two heaters in series. For all practical purposes, sample 49-1 becomes normal at a field greater than 0.2T. On the

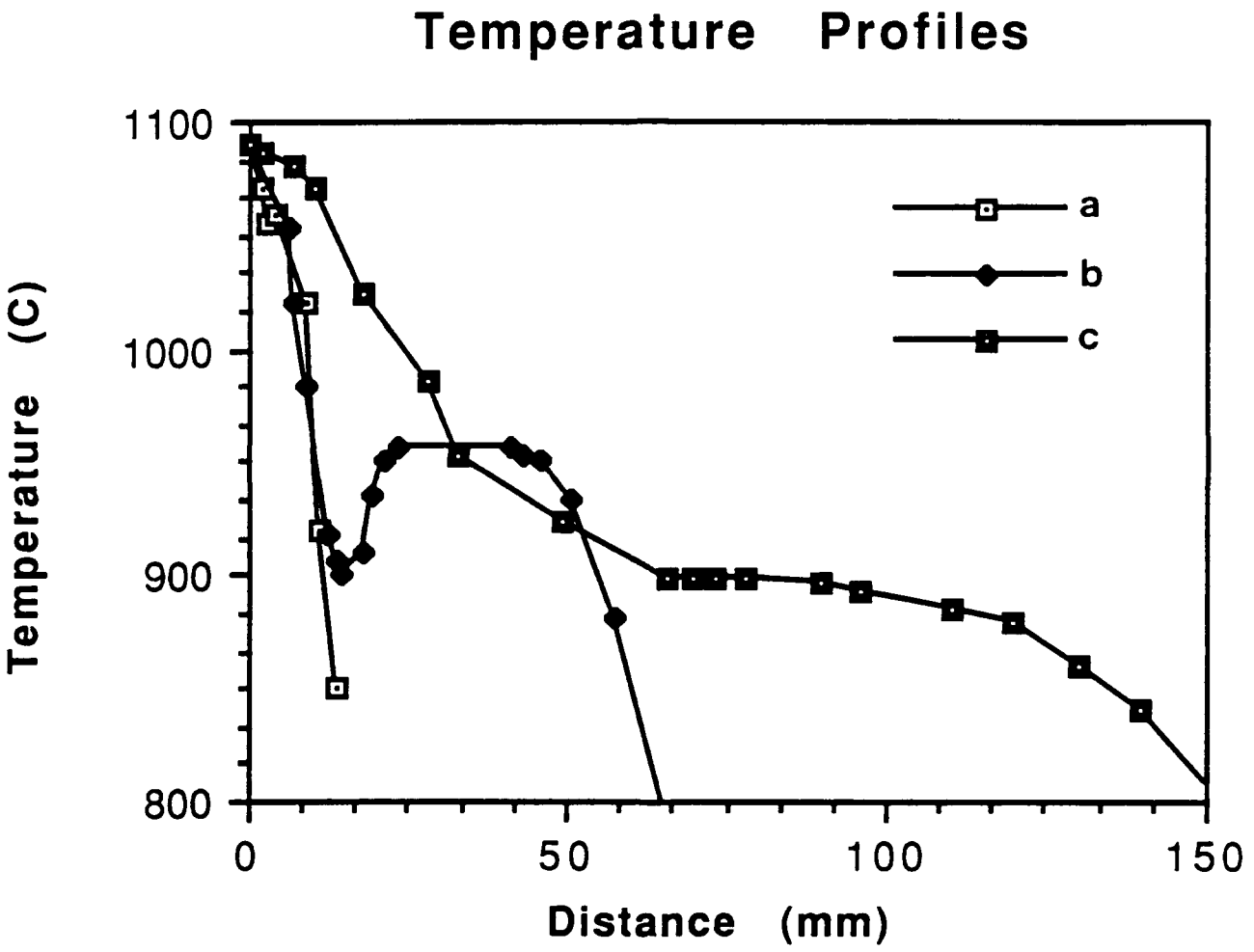

Fig. 8. Temperature profiles used for melt-texturing superconductor fibers. The three curves represent (a) the IR furnace, (b) the double zone furnace, and (c) the gradual cooling furnace.

Fig. 9. $YBa_2Cu_3O_{7-x}$ fiber melt textured along the temperature profile (a) of Fig. 8. Note the high degree of porosity.

GENERAL ATOMICS

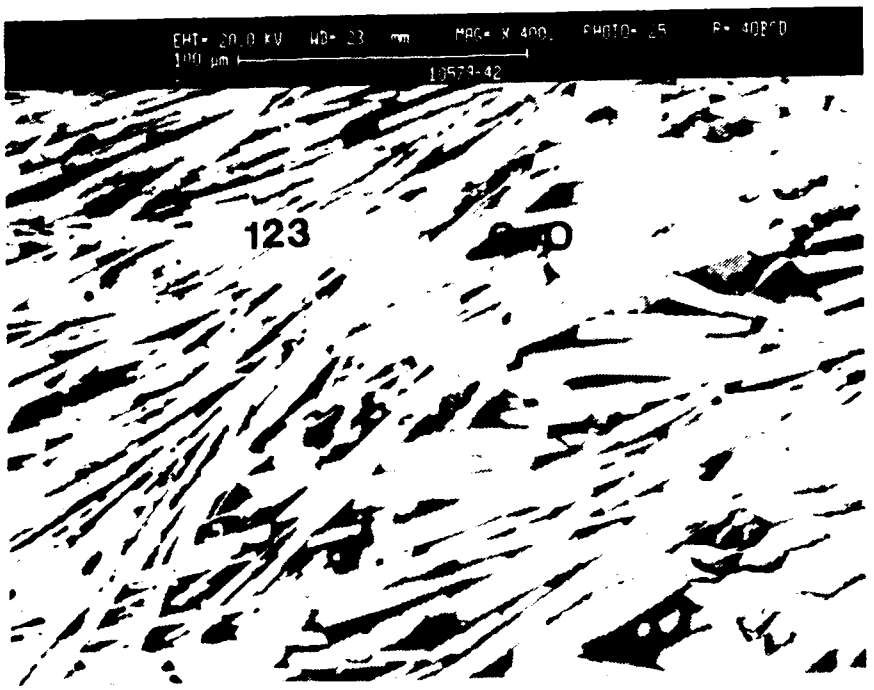

Fig. 10. Backscattered electron image of the fiber shown in Fig. 9. Note the presence of CuO between grain boundaries.

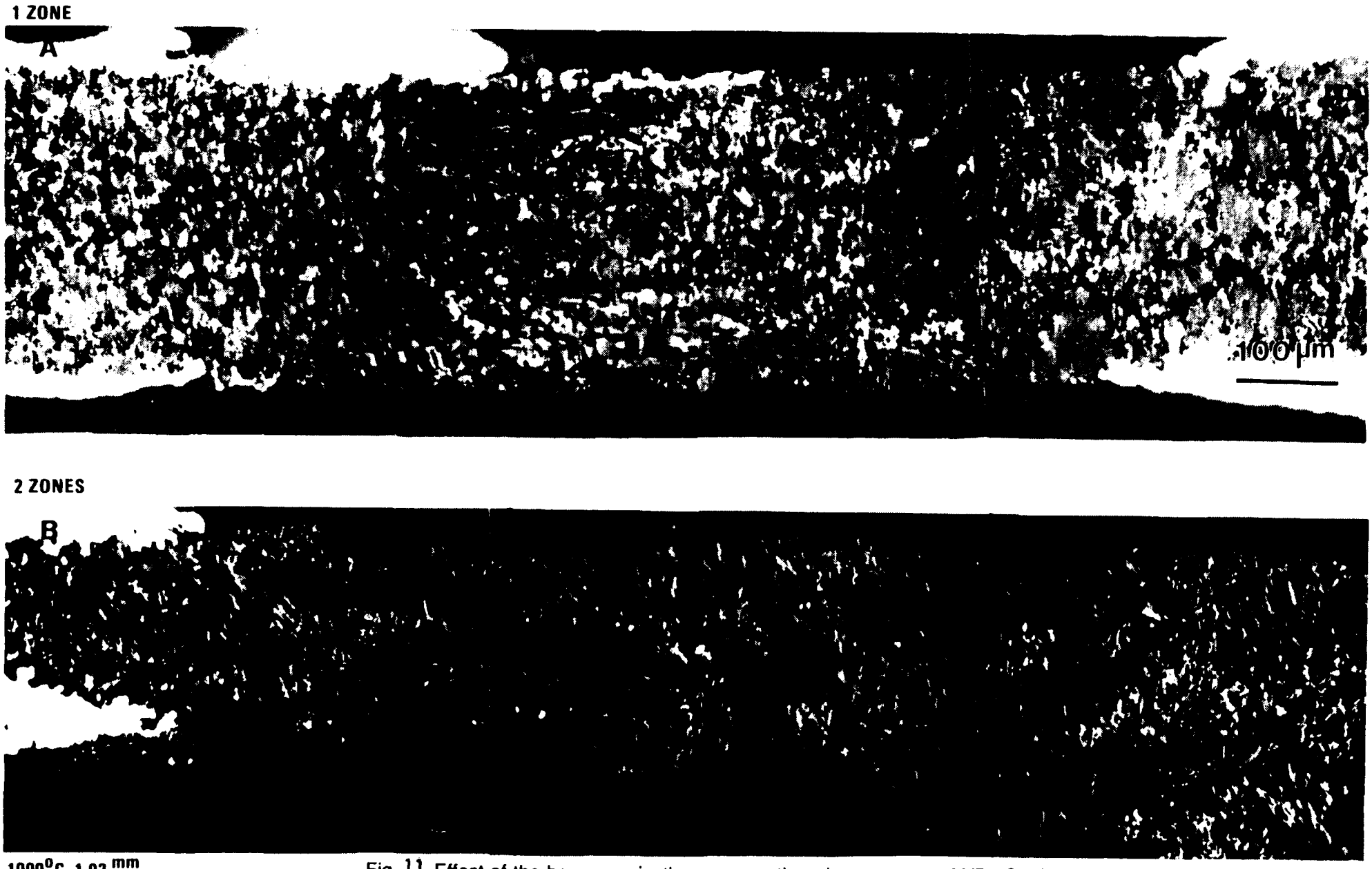

1090°C, 1.02 $\frac{mm}{min}$

Fig. 11. Effect of the homogeneization zone on the microstructure of $YBa_2Cu_3O_{7-x}$

GENERAL ATOMICS

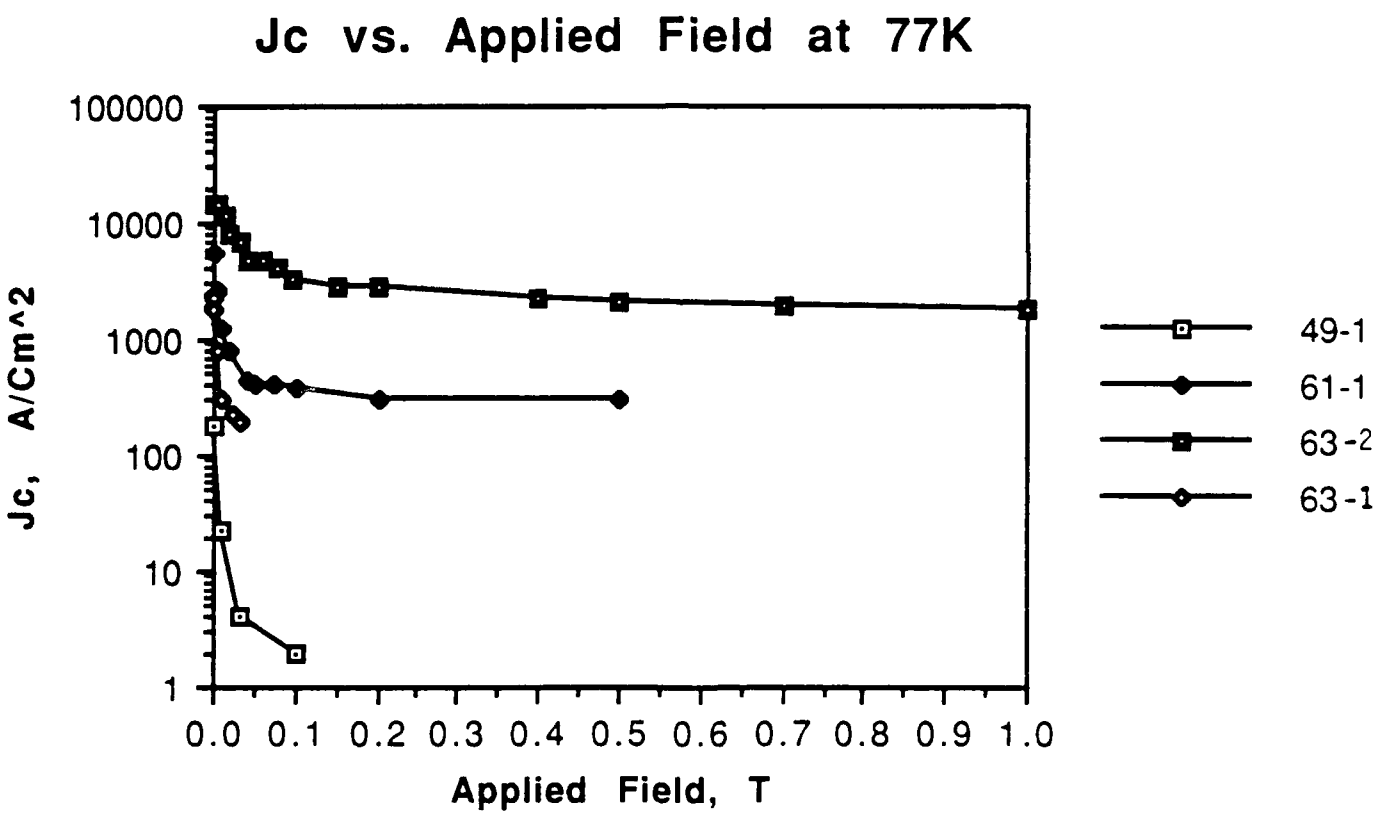

Fig. 12. Critical current densities of melt-textured fibers.

other hand, fiber 61-1 is strongly linked and can pass more than 200 A/cm^2 at 0.5T.

At a speed of nearly 0.1 mm/min, the effect of the secondary heater on fiber microstructure is still the same, but less significant as shown by Fig. 13. Both samples are well aligned and contain small amounts of porosity. Except for a larger grain size of the bottom sample, no significant difference can be seen. However, a drastic difference in J_c performance results. As shown by curve 63-2 of Fig. 14, the fiber melt-textured with the secondary heater, can pass as much as 2000 A/cm^2 up to 1 T, while the fiber melt textured at the same rate using a single heater (curve 63-1) still displays the weak link behavior. The $2X10^3$ A/cm^2 in a field of 1 T is quite comparable to some of the best results reported in the literature for the solid state produced Y123 materials, but more importantly, we were able to obtain this result at a rate nearly twice the speed of other known investigators. Although we, at GA, believe the melt texturing speed is not sufficiently fast enough, it shows promise in that faster processing is possible by simple furnace design improvements.

A-5 CONCLUSIONS

Highly aligned, low porosity $YBa_2Cu_3O_{7-x}$ fibers that can carry up to 2000 A/cm^2 under an applied magnetic field of >1 T have been processed by melt-texturing presintered sol-gel derived fibers through two furnaces in series. The melt-texturing rate of 0.082 mm/min is relatively slow, yet is nearly twice the speed at which the comparable quality samples that are reported in the literature are being processed.

Fig. 13. $YBa_2Cu_3O_{7-x}$ fibers melt textured at 0.082 mm/min through temperature gradient a (upper micrograph) and b (lower micrograph).

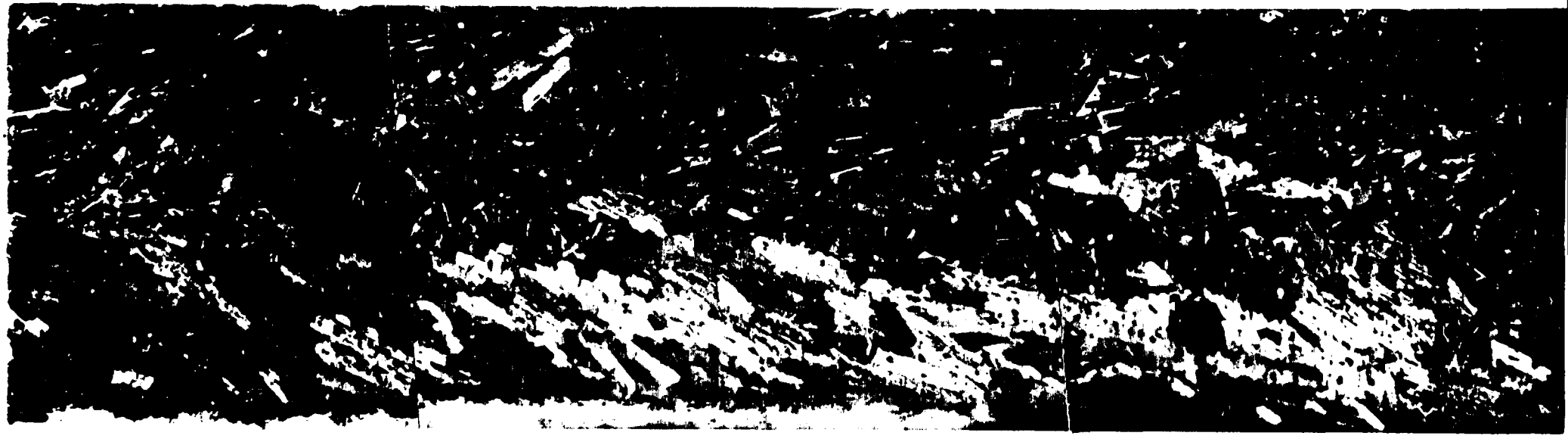

Fig. 14. $YBa_2Cu_3O_{7-x}$ fibers melt textured at 0.082 mm/min through temperature gradient c.

REFERENCES

1. S. Jin, T.H. Tiefel, R.C. Sherwood, M.E. Davis, R.B. van Dover, G.W. Kammlott, R.A. Fastnacht, and H.D. Keith, "High Critical Currents in Y-Ba-Cu-O Superconductors," Appl. Phys. Lett., 52 [24] 2074-2076 (1988).

2. K. Salama, V. Selvamanickam, L. Gao, and K. Sun, "High Current Density in Bulk $YBa_2Cu_3O_x$ Superconductor," Appl. Phys. Lett., 54 [23] 2352-2354 (1989).

3. J. Orehotsky, H. Wiesmann, A.R. Moodenbaugh, M. Suenaga, H.G. Wang, and H. Herman, "Microstructures and dc Critical Currents in Textured Y-Ba-Cu-Oxides," IEEE Trans. Mag., 27 [2] 914-916 (1991).

4. H. Wang, H. Herman, H.J. Wiesmann, Y. Zhu, Y. Xu, R.L. Sabatini, and M. Suenaga, "Texture Growth Processing of Plasma-Sprayed Y-Ba-Cu-O Superconducting Deposits," Appl. Phys. Lett., 57 [23] 2495-2497 (1990).

5. K. No, D.S. Chung, and J.M. Kim, "Fabrication of Textured $YBa_2Cu_3O_x$ Superconductor Using Directional Growth," J. Mater. Res., 5 [11] 2610-2612 (1990).

6. T. Asselage and K. Keefer, "Liquidus Relations in Y-Ba-Cu Oxides," J. Mater. Res., 3 [6] 1279-1291 (1988).

7. J. Kase, J. Shimoyama, E. Yanagisawa, S. Kondoh, T. Matsubara, T. Morimoto, and M. Suzuki, "Preparation of Y-Ba-Cu-O Superconductors with High Critical Current Density by Unidirectional Melt Solidification," Jpn. J. Appl. Phys., 29 [2] L277-L279 (1990).

8. R.L. Meng, C. Kinalidis, Y.Y. Sun, L. Gao, Y.K. Tao, P.H Hor, and C.W. Chu, "Manufacture of Bulk Superconducting $YBa_2Cu_3O_{7-\delta}$ by a Continuous Process," Nature, 345 326-328 (1990).

9. D. Shi, M.M. Fang, J. Akujieze, M. Xu, J.G. Chen, and C. Segre, "High Critical Current Density in Grain Oriented Bulk $YBa_2Cu_3O_{7-x}$ Processed by Partial Melt Growth," Appl. Phys. Lett., 57 [24] 2606-2608 (1990).

10. Z. Lian, "The Melt Process for Fabrication of High Jc YBCO Superconductor," 1991 TMS Ann. Mtng., 3rd Int. Symp. on High-Temp. Supercond.: Processing and Microstructure Relationships, New Orleans, LA, Feb. 17-21, 1991.

11. K. Chen, S.W. Hsu, T.L. Chen, S.D. Lan, W.H. Lee, and P.T. Wu, "High Transport Critical Currents and Flux Jumps in Bulk $YBa_2Cu_3O_{7-x}$ Superconductors," Appl. Phys. Lett., 56 [26] 2675-2677 (1990).

12. P.J. McGinn, W. Chen, and N. Zhu, "Texturing of by $YBa_2Cu_3O_{6+x}$ by Melt Processing," to be published.

13. M. Murakami, M. Morita, K. Doi, and K. Miyamoto, "A New Process with the Promise of High Jc in Oxide Superconductors," Jpn. J. Appl. Phys., 28 [7] 1189-1194 (1989).

14. M. Murakami, M. Morita, N. Koyama, "Magnetization of a $YBa_2Cu_3O_7$ Crystal Prepared by the Quench and Melt Growth Process," Jpn. J. Appl. Phys., 28 [7] L1125-L1127 (1989).

15. M. Murakami, S. Gotoh, H. Fujimoto, N. Koshizuka, and S. Tanaka, "Comparative Study of Flux Pinning, Creep and Critical Currents Between YBaCuO Crystals with and without Y_2BaCuO_5 Inclusions," paper presented at AMSAHTS 90, April 2-6, 1990, Greenbelt, MD.

16. Z. Lian, Z. Pingxiang, J. Ping, W. Keguang, W. Jingrong, W. Xiaozu, "High Jc YBCO Superconductors Prepared by the Powder Melting Process," IEEE Trans. Mag., 27 [2] 912-913 (1991).

17. S. Nagaya, M. Miyajima, I. Hirabayashi, Y. Shiohara, and S. Tanaka, "Rapid Solidification of High-Tc Oxide Superconductors by a Laser Zone Melting Method," IEEE Trans. Mag., 27 [2] 1487-1494 (1991).

APPENDIX II

MATERIALS RESEARCH SOCIETY SYMPOSIUM PROCEEDINGS VOLUME 169

High-Temperature Superconductors: Fundamental Properties and Novel Materials Processing

Symposium held November 27-December 2, 1989, Boston, Massachusetts, U.S.A.

EDITORS:

David Christen
Oak Ridge National Laboratory, Oak Ridge, Tennessee, U.S.A.

Jagdish Narayan
North Carolina State University, Raleigh, North Carolina, U.S.A.

Lynn Schneemeyer
AT&T Bell Laboratories, Murray Hill, New Jersey, U.S.A.

HIGH T_c SUPERCONDUCTOR FIBERS FROM METALLO-ORGANIC PRECURSORS

K.C. CHEN AND K.S. MAZDIYASNI
General Atomics, PO Box 85608, San Diego, CA 92138-5608

ABSTRACT

Homogeneous solution for Y-Ba-Cu-O superconductor was prepared from yttrium i-propoxide, barium i-propoxide, and copper ethylhexanoate. The solution was converted to a resin-like material and was readily dissolved in organic solvents. The resin possesses a cohesive property in a number of solvents, such as benzene and xylene. Single-phase superconducting $YBa_2Cu_3O_{7-x}$ fibers have been continuously spun from the viscous solution. Controlled amounts of Y_2BaCuO_5 phase in the fibers were made possible by slight adjustments in the solution compositions. Partial substitution of copper ethylhexanoate with copper trifluoroacetate prevents barium carbonate formation in the fiber during curing and organic pyrolysis.

INTRODUCTION

For the new high T_c superconducting ceramics to be useful, they must be made into desirable shapes. Specifically, the magnetic applications critically depend on the fabrication of fibers or tapes that carry sufficiently high electrical current. Fabrication of $YBa_2Cu_3O_{7-x}$ superconductor ceramic fibers or wire with adequate strength, modulus, and electromagnetic properties is a formidable task because the yttrium barium cuprate ceramic material is brittle and is not easily drawn into the desirable fine fiber geometry. Such fiber property requirements demand high chemical and phase purities as well as crystallographic orientation in the a or b direction, uniform microstructure, and clean grain boundaries.

Various methods have been used to prepare superconducting fibers [1]. The powder-in-binder [2], powder-in-sol [3], sol-gel and metallo-organic [4-8] methods adopt the spinning process, which has been established for ceramic fiber-making. In this paper, we discuss the method involving the preparation of single phase $YBa_2Cu_3O_{7-x}$ fibers and fibers with minor Y_2BaCuO_5 phase inclusions from metallo-organic precursors. We also describe modification of the solution chemistry to overcome barium carbonate formation.

EXPERIMENTAL PROCEDURES

Yttrium i-propoxide/i-propanol solution was prepared by the method described by Mazdiyasni, et al. [9]. Barium i-propoxide/i-propanol solution was prepared by reacting barium metal chips (Alfa Products) with dry i-propanol. Copper ethylhexanoate/i-propanol solution was made by dissolving copper ethylhexanoate (Alfa Product) in dry i-propanol. Copper trifluoroacetate was synthesized by reacting copper ethoxide (Alfa Products) with trifluoroacetic acid.

Stoichiometric ($YBa_2Cu_3O_{7-x}$) or off-stoichiometric ($YBa_2Cu_3O_{7-x}$ + y Y_2BaCuO_5) solutions were obtained by pipetting the calculated volumes from each stock solution. In cases where copper trifluoroacetate were used, 2/3 to 1 mole of copper trifluoroacetate per mole of yttrium was added to partially substitute for copper ethylhexanoate. A green precipitate formed when copper solution was introduced. This precipitate was hydrolyzed by adding water/isopropanol solution. The greenish precipitate gradually dissolved after adding water, and a clear dark green solution formed. This

Mat. Res. Soc. Symp. Proc. Vol. 169. © 1990 Materials Research Society

solution was further concentrated in a vacuum oven or a rotary evaporator until it became highly viscous liquid or completely dry resin-like mass. The dried resin could be dissolved to a prescribed viscosity in a number of solvent mixtures, such as benzene-isopropanol or xylene-isopropanol solutions. Fibers were prepared either by hand-drawing or mechanical spinning from these viscous liquids.

RESULTS AND DISCUSSIONS

The dry resin is readily dissolved or "softened" by using proper ratios of benzene-isopropanol mixtures. The characteristics of the resin in these solutions are shown in Figure 1. There are several regions in this ternary phase diagram. Transitions across boundaries are gradual. The transition between regions is reversible and can be done by adding or removing solvents. In the low benzene, low isopropanol region (region V), the resin becomes viscous. Within this region, fibers can be easily prepared by hand-drawing or mechanical spinning (Figure 2). In the high isopropanol region (region P), precipitation occurs. In region L_c, a solution with a very small amount of colloid exists. A stable solution can be obtained in region L. Similar results were observed in a xylene-isopropanol system.

In the tie line between the benzene-resin, resins possess an interesting cohesive property, i.e., they do not stick to glass vials. This property enables resins to be molded into different shapes (Figure 3). The fibers spun from the resin have adequate mechanical strength prior to pyrolysis and sintering and are flexible. After calcination, some fibers of 20 microns diameter were able to be bent into a circle of 1 to 2 cm radius.

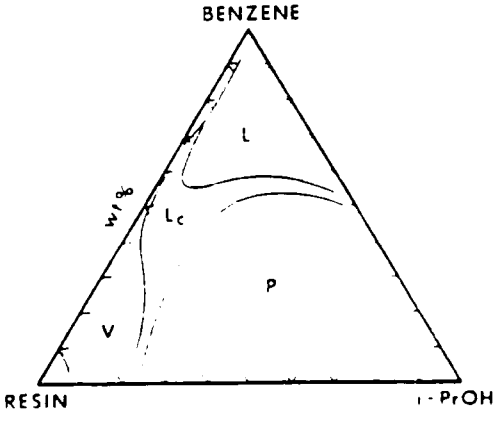

Figure 1. Characteristics of the "123" resin in binary benzene-i-propanol mixtures. (see text for legends)

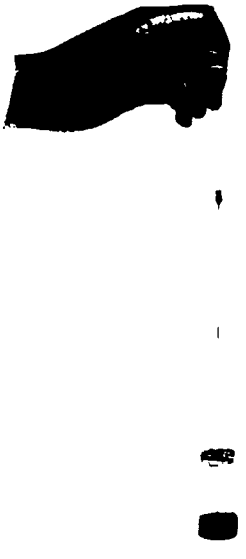

Figure 2. Preceramic fibers drawn from viscous solutions.

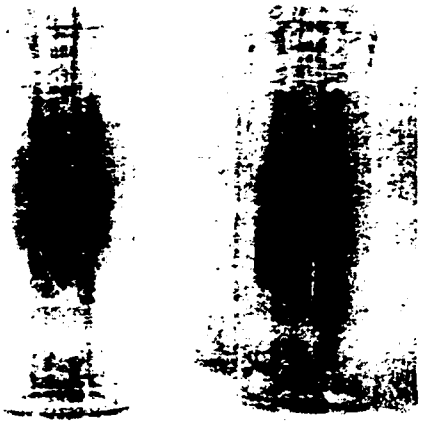

Figure 3. Cohesive property of resin in benzene enables it to be molded into different shapes.

The phase purity of the fibers was examined by X-ray and DTA. The X-ray indicates only single phase $YBa_2Cu_3O_{7-x}$ in the fiber. By using DTA, no low-melting impurities at 950°C were observed in the fibers [Figure 4(a)]. In order to obtain a controlled amount of fine Y_2BaCuO_5 phase in the fibers for possible flux pinning centers, the stoichiometry of the solutions was slightly adjusted so that the final compositions of the fibers were in the tie line between $YBa_2Cu_3O_{7-x}$ ("123") + y Y_2BaCuO_5 ("211"). Figures 4(b) and (c) show X-ray and DTA curves with y values equal to 0.02 and 0.05. The ease of tailoring the phase in the fibers by the metallo-organic process is clearly demonstrated.

The dc magnetic susceptibility of the fiber indicated the T_c onset is 87K. The electrical resistivity measurement shows the fibers have T_c (R = 0) at 81K (Figure 5).

Prevention of stable barium carbonate formation was achieved by partial substitution of copper ethylhexanoate with copper trifluoroacetate. During heat treatment, barium fluoride formed in the fibers instead of usual barium carbonate (Figure 6). The fibers containing barium fluoride were converted to "123" phase by calcining them at 850°C for 18 hr in flowing oxygen saturated with water vapor and then switching to dry oxygen at 900°C for 10 to 24 hr.

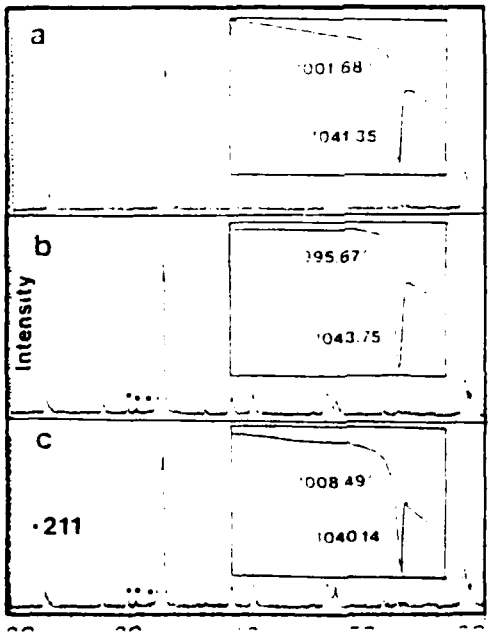

CONCLUSIONS

Superconducting fibers were prepared from a soluble resin derived from metallo-organic precursors. The resin becomes either viscous, fluid, or precipitate in different benzene-isopropanol mixtures and is cohesive in benzene. Single-phase $YBa_2Cu_3O_{7-x}$ fibers with T_c (R = 0) = 81K were obtained. Substitutions of copper ethylhexanoate with copper trifluoroacetate prevents barium carbonate formation during calcination of the fibers.

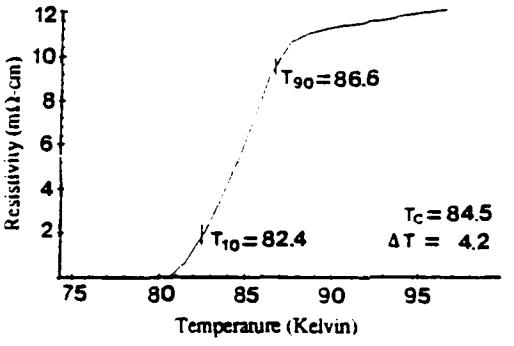

Figure 5. Electrical resistivity of the fibers calcined at 900°C for 12 hr and annealed at 450°C for 24 hr.

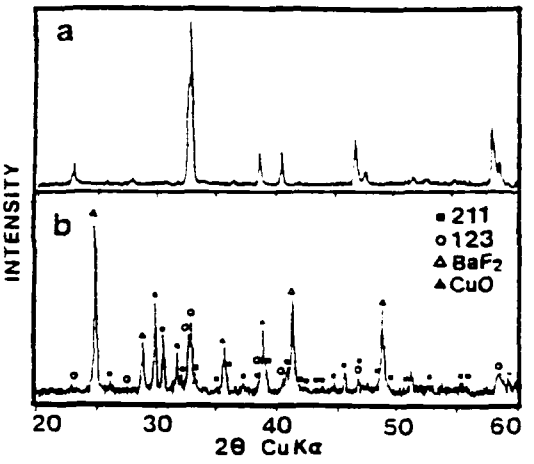

Figure 6. No $BaCO_3$ formation during the pyrolysis of trifluoroacetate containing preceramic fibers.

REFERENCES

1. T.H. Tiefel, et al., J. Appl. Phys. 64, 5896 (1988).
2. R. Goto and M. Kada, J. Mater. Res. 3, 1292 (1988).
3. R. Enomote, et al., Japan. J. Appl. Phys. 28, L1207 (1989).
4. T. Umeda, H. Kozuka, and S. Sakka, Advanced Ceramic Materials 3, 520 (1988).
5. J.C.W. Chien and M.M. Gong, Phys. Rev. B. 38, 11.853 (1988).
6. H. Konishi, T. Takamura, H. Kaga, and K. Katsuse, Japan. J. Appl. Phys. 28, L241 (1989).
7. R. M. Laine, et al., in Ceramic Superconductors II edited by M.F. Yan (Amer. Ceram. Soc., Westerville, Ohio, 1988) pp. 450-463.
8. H. Zheng, et al., in High Temperature Superconductor II edited by D.W. Capone II, W. H. Butler, B. Barlogg, and C.W. Chu (Material Res. Soc. 1988) Extended Abstract 93 (1988).
9. K.S. Mazdiyasni and L.M. Brown, Inorg. Chem. 9, 2783 (1970).

MATERIALS RESEARCH SOCIETY SYMPOSIUM PROCEEDINGS VOLUME 180

Better Ceramics Through Chemistry IV

Symposium held April 16-20, 1990, San Francisco, California, U.S.A.

EDITORS:

Brian J.J. Zelinski
University of Arizona, Tucson, Arizona, U.S.A.

C. Jeffrey Brinker
Sandia National Laboratories, Albuquerque, New Mexico, U.S.A.

David E. Clark
University of Florida, Gainesville, Florida, U.S.A.

Donald R. Ulrich
Air Force Office of Scientific Research, Washington, D.C., U.S.A.

MRS MATERIALS RESEARCH SOCIETY
Pittsburgh, Pennsylvania

METALLO-ORGANICS DERIVED TRACTABLE RESINS FOR YBCO SUPERCONDUCTING FIBER FABRICATION

K.C. Chen, A. Y. Chen and K. S. Mazdiyasni
General Atomics, PO Box 85608, San Diego, CA 92138-5608

ABSTRACT

Soluble resins were prepared by controlled hydrolysis of yttrium isopropoxide, barium isopropoxide and copper ethylhexanoate. The resins were converted to cohesive, viscous, fluid and precipitated states by the addition of different combinations of binary polar and non-polar organic solvents. Viscosity and spinnability of the resins were critically dependent on the solvent constituents. Continuous pre-ceramic fibers were spun from these resins and single phase $YBa_2Cu_3O_y$ superconducting fibers with T_c=91.5K and ΔT=1.5K have been obtained.

INTRODUCTION

The magnetic applications of a superconducting cable require high critical currents, strengths and modulus of the superconducting fibers. To meet these requirements, the fiber must have the following features: chemical stoichiometry, phase purity, high density, crystallographic orientation in the c direction, uniform fine microstructure and clean grain boundaries.

There are few known methods for fabricating superconducting fibers of 20-100 μm in diameter without an outer cladding or center wire as support. These methods include metal-alloy, powder-in-binder [1], powder in sol [2], sol-gel and metallo-organics [3-7]. In order to spin fibers directly from the metallo-organic derived resins, the resin not only has to meet the requirements for the final ceramic fiber, but must also have high viscosity, viscoelasticity, cohesiveness, green strength, low shrinkage and high oxide content. In this paper, we discuss the preparation of metallo-organic derived tractable resins that possess several key parameters of the aforementioned properties for continuous spinning of single phase $YBa_2Cu_3O_y$ fibers.

EXPERIMENTAL PROCEDURE

Yttrium isopropoxide/isopropanol solutions, barium isopropoxide/isopropanol solution and copper ethylhexanote/isopropanol stock solutions were prepared as described previously [8]. Solutions containing stoichiometric ($YBa_2Cu_3O_y$) amounts of required elements were prepared by pipetting the calculated volume from each stock solution into a 500 ml three-neck round bottom flask. First, barium isopropoxide and yttrium isopropoxide were mixed, and a clear yellowish solution was obtained. A green precipitate formed when copper ethylhexanoate solution was later introduced. This solution was refluxed gently in a dry nitrogen atmosphere for 2 hours. This precipitated solution was then hydrolyzed by adding a mixture of water/isopropanol, using 10 equivalents of water per mole of yttrium isopropoxide while the solution temperature was kept at 50-60°C. The greenish precipitate dissolved after adding water and a clear dark green solution formed. This solution was concentrated and initially dried in a rotary evaporator, was further dried in a vacuum oven and was then ground into powder for storage. Suitable viscosity could be achieved when the dried powder was dissolved with the proper amounts of several binary solvent mixtures, such as benzene-isopropanol, hexane-isopropanol, toluene-isopropanol and xylene-isopropanol. The fibers were then prepared by mechanical spinning from the cohesive mass.

RESULTS AND DISCUSSIONS

Behavior of the resin in different binary solvents

A number of processing parameters, including the amount of water added, temperature and time were critical to the formation of viscous resins. Low water ratios and low bath

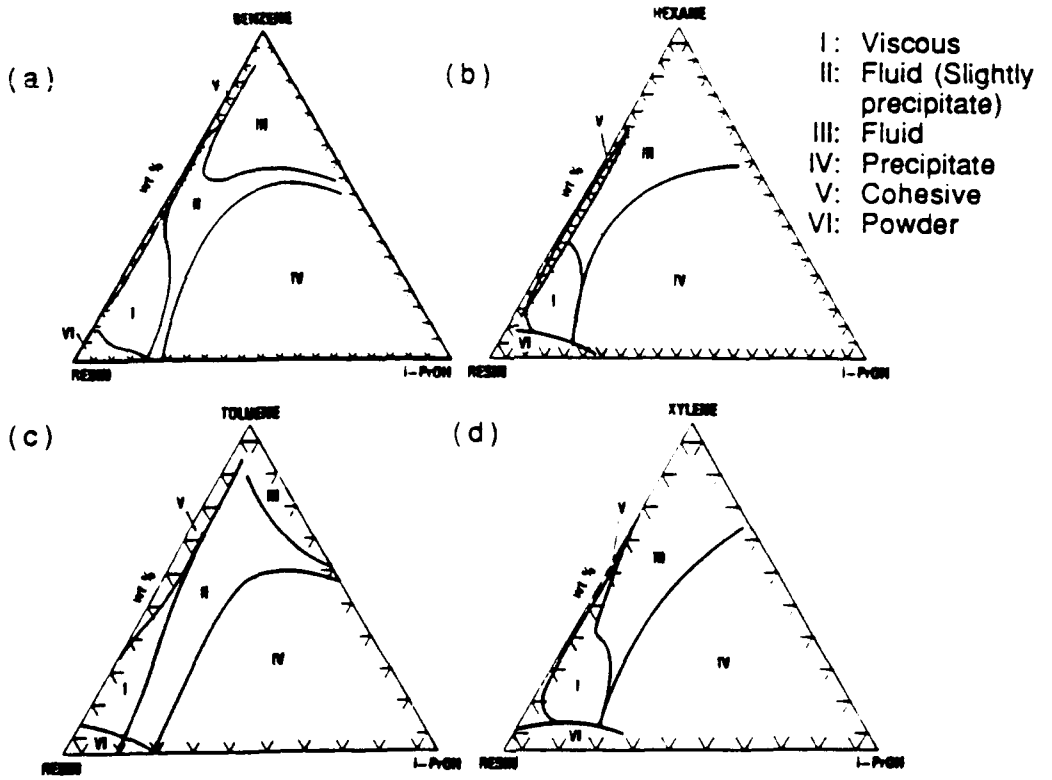

Figure 1. The characteristics of Y123 resins in binary solvent systems, (a) benzene-isopropanol; (b) hexane-isopropanol; (c) toluene-isopropanol and (d) xylene-isopropanol

temperatures prolonged the time needed for dissolving the green precipitate. Prolonged heating or refluxing after water addition caused precipitation in the solution that resulted in composition fluctuation within the resin.

The resins were stored in dry powder form that extended their shelf life and provided flexibility for processing. The dry resin powder was readily dissolved or "softened" by using proper ratios of benzene-isopropanol, hexane-isopropanol, toluene-isopropanol and xylene-isopropanol. The behaviors of the resin in these binary solutions are shown as a function of weight percentage in the ternary diagrams. (Figures 1 (a)-(d)). There are several regions of interest in these ternary diagrams.

In general, the viscosity of the resin solutions decreased with increasing amounts of either benzene or isopropanol in regions I, II, and III. In low benzene, low isopropanol region I, the resin became highly viscous and did not immediately flow when the glass vial was inverted. Fibers could be prepared by hand-drawing only within a small area in region I. Similar behavior was also observed in region I of the other systems. In regions II and III, the solutions instantaneously flowed when glass vials were tilted. Therefore, regions II and III were described as fluid regions in contrast to the non-flowing region I (viscous region). Region II had a very small amount of precipitation. The viscosity at the boundary between region I and III was approximately 10^6 mPa·s. Stable solutions were obtained throughout region III.

In region IV, which contained more isopropanol, massive precipitation occurred. The amount of the precipitation increased with increasing isopropanol. The resins were cohesive in region V and on the tie-line between resin and non-isopropanol solvents, except in hexane-isopropanol system. The resins did not stick to glass vials. This property enabled them to be molded or extruded into different shapes. The resin had a tendency to expel excess solvents that could co-exist as clear solution with the cohesive resin mass. The critical solvent contents for solvent separation were around 60-70 w% of benzene, toluene or xylene. In region VI, there was an insufficient amount of solvent to completely wet the resin. The transitions across the regional boundaries were gradual, but the transitions between the regions were reversible and could be done by solvent addition or removal. This reversibility greatly simplified the preparation of resins with optimal fiber spinnability.

Table 1. Characteristics of resins in benzene-isopropanol binary solvents.

Test Run	Resin constituents (wt%)			Resin Characteristics				
	C_6H_6	i-PrOH	Dry Resin	Cohesive	Surface Smoothness	Die Swell	Flexibility	Collapse
B1	26.8	0.0	73.1	yes	no	slight	some	no
B2	48.3	2.6	49.1	yes	yes	slight	yes	yes
B3	39.6	2.2	58.3	no	yes	large	yes	yes
B4	25.4	1.4	73.2	yes*	yes	large	yes	yes
B5	30.3	1.1	68.5	yes*	yes	no	yes	yes
B6	20.0	1.0	78.9	yes*	yes	large	yes	yes
B7	18.8	1.0	81.2	yes*	yes	no	yes	slight
B8	17.8	1.0	80.2	yes	yes	no	yes	no

* Slightly tenacious.

Spinning of precursor fibers

The viscosity of the resins was adjusted by mixing the dry resin powder with the required amounts of the solvents immediately before spinning. The resins could be dry-spun because of their cohesiveness, viscoelasticity and high viscosity. The elongational viscosity rapidly increased after extrusion from the nozzle as a result of solvent evaporation.

The viscosity of the viscous resins in the fiber drawing regions (regions I and V) was at least 10^6 mPa.s. Because of the cohesive property of the resins, the fiber retained the shape of the spinneret and readily wound onto the pick-up wheel. The viscoelasticity enabled the resin to be drawn to 1/10 to 1/3 of the opening of the nozzle. The viscosity, cohesiveness and viscoelasticity of the resin were very sensitive to the solvent constituents. Solvent contents in the resin also greatly influenced other fiber spinning properties, such as die-swelling, surface smoothness, flexibility, modes of fracture (brittle vs. ductile), collapsing and extrusion pressures. Table 1 gives the resin characteristics as a function of solvent contents in benzene-isopropanol systems. Figure 2 shows the effect of the solvent content on die-swelling and collapsing. With proper solvent composition, precursor fibers of 50-1000 μm in diameter were easily spun (Figure 3). Thin fibers were flexible and had sufficient green strength for handling.

Conversion of the resin into superconducting ceramic fibers

The dry resins and as-drawn fibers were X-ray amorphous. Calcination of the resin at 400-750°C resulted in mixed phases of Y_2CuO_5, $BaCO_3$ and CuO. $YBa_2Cu_3O_y$ phase appeared at 750°C. After 1 to 4 hours at 800°C, there were substantial amounts of $YBa_2Cu_3O_y$ with small amounts of Y_2BaCuO_5 and $BaCuO_2$ phases present. At 900°C for 1 to 8 hours, single phase $YBa_2Cu_3O_y$ was obtained. DTA run in dry nitrogen showed no low melting impurity phases at 950°C in these fibers [8]. Fibers having T_c =91.5K with ΔT=1.5K were obtained after heat treatment of 950°C for 15 hours followed by a 24-hour anneal at 400°C (Figure 4).

CONCLUSIONS

Suitable metallo-organic precursors were synthesized and processed to prepare tractable resins for YBCO fiber fabrication. These resins became cohesive, viscous, fluid or precipitated in several binary solvent systems. The spinnability of the resins was controlled by the amount of solvent constituents. Continuous precursor fibers were successfully spun from the resins. Superconducting fibers with T_c =91.5K and ΔT=1.5K were obtained.

ACKNOWLEDGEMENTS This research was supported by DARPA/ONR. The electrical properties were measured by Ms. Lisa Paulius and Dr. Patti Tsai of Physics Department, UCSD.

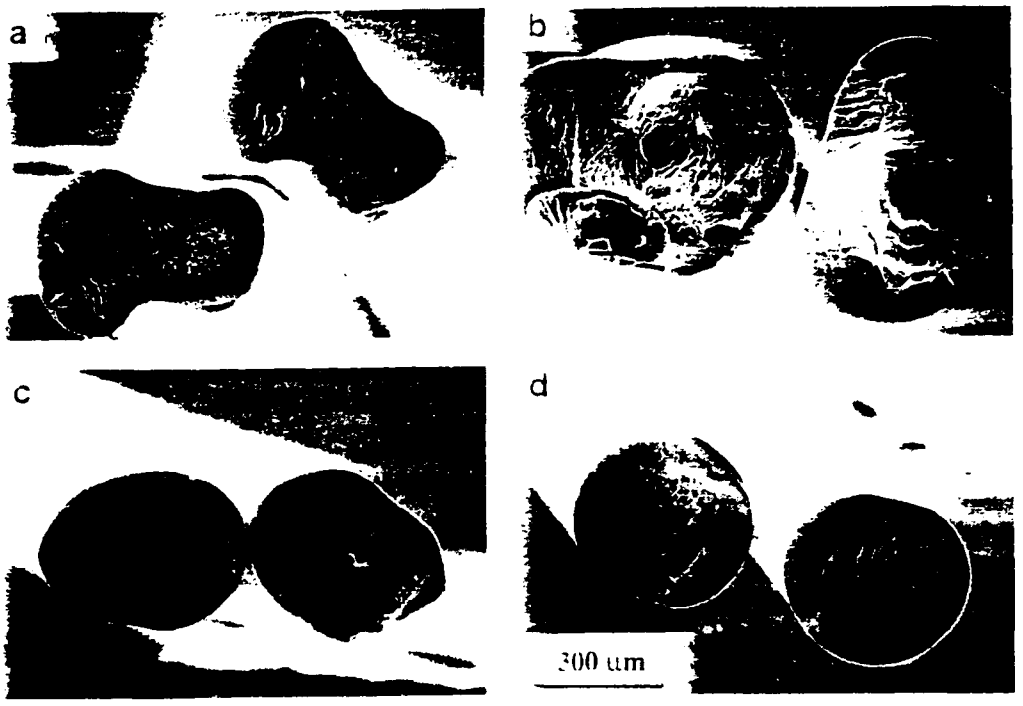

Figure 2. Precursor fibers morphology with different degrees of die-swelling and collapsing: (a) sample B5: no die-swelling, large collapsing; (b) sample B6: large die-swelling, medium collapsing; (c) sample B7: no die-swelling, medium collapsing and (d) sample B8: no die-swelling, no collapsing.

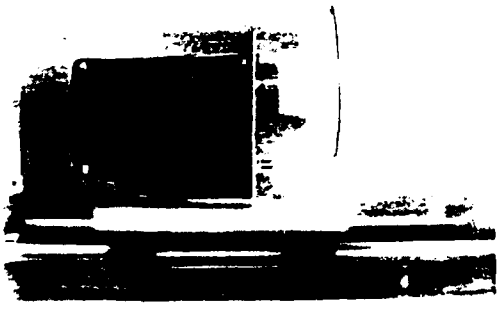

Figure 3. Continuous precursor fiber was prepared by dry-spinning of the resins.

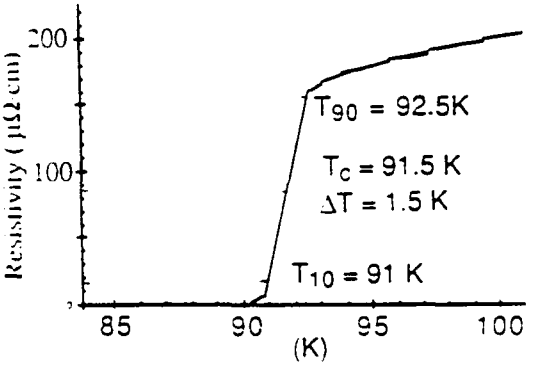

Figure 4. Resistivity of superconducting fiber calcined at 950°C for 15 hours and annealed at 400°C for 24 hours.

REFERENCES

1 T. Goto and M. Kada, J. Mater. Res. 3, 1292 (1988).
2. R. Enomoto et al., Japan. J. Appl. Phys. 28, L1207 (1989).
3. T. Umeda, H. Kozuka, and S. Sakka, Advanced Ceramic Materials 3, 520 (1988)
4. J. C. W. Chien et al. Phys. Rev B 38, 11-835 (1988).
5. H. Konishi, T. Takamura, H. Kaga and Katsuse, Japan. J. Appl. Phys. 28, L241 (1989).
6. F. Uchikawa and J. D. Mackenzie, J. Mater. Res. 4, 787 (1989).
7. M.W.Rupich, S. F. Cogan, B. Lagos and J. P. Hachey, Mater Res. Soc. Meeting, Fall 1989 Boston, MA, USA (to be published in MRS Proceeding).
8 K. C. Chen and K. S. Mazdiyasni, Mater. Res. Soc. Meeting, Fall 1989, Boston, MA. (to be published in MRS Proceeding).

Flux bundle interactions

Richard B. Stephens
General Atomics, San Diego, California 92121

(Received 22 May 1990; accepted 29 August 1990)

We show that magnetic flux lattice interactions are important at fields above a few thousand gauss. These interactions interfere with thermally activated current-induced flux bundle hopping and reduce the superconductor's flux creep resistance below that estimated from the standard flux creep models (which assume completely independent hopping). We find that the flux bundles can hop independently at the low fields at which, e.g., antennas and SQUID detection coils would be used, but interact very strongly at fields typical of magnet applications.

I. INTRODUCTION

Flux creep, which is hard to detect in older type II superconductors,[1,2] is apparently the dominant effect in limiting the current-carrying capability of the ceramic oxide superconductors.[3] Their shorter coherence length leads to a weaker flux pinning energy, while operation at higher temperatures gives the flux bundles considerably more thermal energy. Thermally activated hopping of flux bundles is therefore much more rapid than in the older materials.

This phenomenon has been analyzed from two very different points of view. A spin glass model was originally proposed.[4] Subsequently, a large number of people have applied the Anderson–Kim model of flux hopping.[5] In the former model, the interaction between flux bundles is so strong that several bundles must move in a coordinated fashion during a relaxation event. The latter model assumes flux bundles interact very weakly and hop independently of their neighbors.

The purpose of this paper is to define the regime for which flux bundle interactions are important, to describe their effect on flux creep resistance, and to delineate the boundaries between the independent hopping, interactive hopping, and coordinated hopping regimes. We conclude that the interaction is strong enough to significantly restrict flux creep over most of the range of conditions for which these superconductors will be used. At fields above 7 T it is sufficiently strong that cooperative multibundle hopping dominates.

II. QUALITATIVE DESCRIPTION

We will define the boundary between cooperative and independent flux hopping using a minimal array of flux bundles—one bundle (containing a quantum of flux) surrounded by a hexagon of six neighboring bundles at the equilibrium distance[6] (in the absence of current).

$$r = a\left(\frac{\Phi_0}{H}\right)^{1/2} \tag{1a}$$

where H is the applied field and $a \approx 1$. For the purposes of this discussion, r is written in terms of the lower critical field,[7] $H_{c1} = \Phi_0 \ln \kappa/4\pi\lambda^2$, and magnetic field penetration length, λ. The Ginsberg–Landau parameter κ is small enough so that it can be ignored, and one can write:

$$r \cong \sqrt{4\pi}\lambda\left(\frac{H_{c1}}{H}\right)^{1/2}. \tag{1b}$$

The flux bundles are pinned, but we assume that the density of pinning sites is so high that that does not modify the position of the flux bundles (separation between pinning sites, d, much less than r) and their hexagonal symmetry is unaffected. We then turn on a transverse current density J. The pinning sites (with pinning energy U), current, and neighbors interact with the central flux bundle to produce a free energy which varies with position, as shown in Fig. 1.

Thermally generated fluctuations cause the flux bundle to periodically jump out of its pinning site. On such a jump the Lorentz force from the current tends to drive the flux bundles to the right, reducing the energy at the right-hand side by $U_J(\mathbf{x}) \equiv \mathbf{J} \times \mathbf{B} \cdot \mathbf{x}$, but interaction with the surrounding lattice, ΔU_{int}, resists those hops. The dynamics of the flux lattice depends on the relative sizes of these three energies, kT, U_J, and ΔU_{int}:

(1) The interaction energy reduces the individual hopping rate when $\Delta U_{int} > kT$ or $U_{int} > U_J$.

(2) The interaction energy reduces the rate of individual hopping to less than that of coordinated hopping of multiple bundles (spin glass behavior) when $\Delta U_{int} > U$.

(3) If $kT > \Delta U_{int}$ even for hopping distances that are a large fraction of the flux bundle lattice constant, then the bundle positions will be essentially random, and the lattice will "melt".

III. FLUX CREEP RESISTANCE

To analyze the effects caused by this interaction, we separate the hopping process into two parts: first

The change in energy for the central flux bundle on a hop of length δr, $\Delta U_{int}(\delta r)$ toward its neighbors, is

$$\Delta U_{int}(\phi, \delta r) = C \sum_{n=0}^{5} \frac{\delta r}{\lambda} \sin\left(\frac{2n\pi}{6} + \phi\right) K_0'(r) + \frac{1}{2}\left[\frac{\delta r}{\lambda} \sin\left(\frac{2n\pi}{6} + \phi\right)\right]^2 K_0''(r) + \cdots$$

$$= C \frac{\delta r}{\lambda} \sum_{n=0}^{5} \sin\left(\frac{2n\pi}{6} + \phi\right) K_0'(r) + \frac{1}{2}\left(\frac{\delta r}{\lambda}\right)^2 \left[\sum_{n=0}^{5} \sin^2\left(\frac{2n\pi}{6} + \phi\right)\right] K_0''(r) + \cdots \quad (10)$$

The higher powers of sin in Eq. (10) can be reduced to first powers of functions of multiples of the argument[10]:

$$\sin^2\phi = \frac{1}{2}(1 - \cos 2\phi)$$

$$\sin^3\phi = \frac{1}{4}(3 \sin \phi - \sin 3\phi)$$

$$\sin^4\phi = \frac{1}{8}(3 - 4 \cos 2\phi + \cos 4\phi)$$

$$\sin^5\phi = \frac{1}{16}(10 \sin \phi - 5 \sin 3\phi + \sin 5\phi)$$

$$\sin^6\phi = \frac{1}{32}(10 - 15 \cos 2\phi + 6 \cos 4\phi - \cos 6\phi)$$

Then by symmetry

$$\sum_{n=0}^{5} \sin(2nm\pi/6 + m\phi) = 0$$

unless m is a multiple of 6 so all the odd terms in the series in Eq. (10) are zero, and the sum reduces to

$$\Delta U_{int}(\phi) = C\left[\frac{3}{2}\left(\frac{\delta r}{\lambda}\right)^2 K_0''\left(\frac{r}{\lambda}\right) + \frac{3}{32}\left(\frac{\delta r}{\lambda}\right)^4 K_0''''\left(\frac{r}{\lambda}\right) + \frac{(10 - \cos 6\phi)}{3840}\left(\frac{\delta r}{\lambda}\right)^6 K_0''''''\left(\frac{r}{\lambda}\right) \cdots\right] \quad (11)$$

so the angular dependence of the interaction energy doesn't appear until the 6th order term.

The limiting forms for $a \equiv r/\lambda \gg 1$ and $\ll 1$, respectively, are:

$$K_0(a) = \left(\frac{\pi}{2a}\right)^{1/2} e^{-a} \quad (12)$$

$$K_0(a) = 0.12 - \ln(a) \quad (13)$$

The flux lattice in a type II superconductor varies from $a \cong 3$ (at H_{c1} where it first penetrates) to $a = \xi/\lambda \approx 0.03$ (at H_{c2} the maximum field). One can see from Fig. 2 that the two analytic forms diverge from $K_0(a)$ at

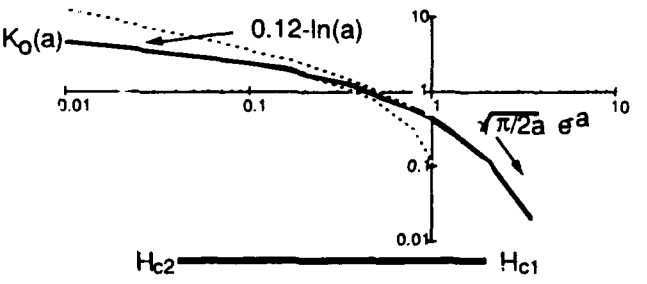

FIG. 2. $K_0(a)$ plotted with its limiting forms for large and small a. The limit of applicability for the asymptotic forms occurs at $a \approx 0.5$. The parameter a varies between 3 and 0.03 as H varies between H_{c1} and H_{c2}.

$a \cong 0.5$—within the region of interest. Within their regimes, the analytic forms have errors of <50%. The first derivatives are continuous at the breakpoint, and the second derivatives different by ≅30%. To avoid problems a power series expansion (which had errors less than 10^{-8} for $a < 2$) was used for calculations of $K_0(a)$ [11] In the discussion below, the limiting form for small a [Eq. (13)] will be used to give a rough idea of the functional form of the equations.

Given a current through the superconductor, there is a transverse force $\mathbf{J} \times \mathbf{B}$ on the flux bundles which tends to force the bundles to the right. This motion is significantly reduced when the increase in interaction energy on a single hop, $\Delta U_{int} > kT$. It is reduced to less than that of cooperative movement of multiple bundles when $\Delta U_{int} > U$. Writing these relations out in detail, the boundaries between independent flux motion and single hopping in a flux lattice, and between single hops and cooperative motion in a flux lattice occur at:

$$T = \frac{C}{k_B}\left[\frac{3}{2}\left(\frac{d}{\lambda}\right)^2 \frac{H}{H_{c1}} + \frac{3}{32}\left(\frac{d}{\lambda}\right)^4 \left(\frac{H}{H_{c1}}\right)^2 \cdots\right] \quad (14)$$

$$U_{pin} = C\left[\frac{3}{2}\left(\frac{d}{\lambda}\right)^2 \frac{H}{H_{c1}} + \frac{3}{32}\left(\frac{d}{\lambda}\right)^4 \left(\frac{H}{H_{c1}}\right)^2 \cdots\right] \quad (15)$$

where d is the distance between pinning sites, λ is the magnetic penetration length, and H_{c1} is the lower critical field.

Note that one can use Eq. (14) to define the distance a flux bundle can move from its equilibrium position, Δ_{kT}, before being affected by its neighbors. It is useful to define this relative to the size of the flux lattice, r. When $\Delta_{kT}/r \geq 0.2$, one might expect the lattice to become so disordered that the model being used here is not useful, so one has a boundary defining the validity limit for this model of

$$T_{melt} = \frac{C}{k_B}\frac{\Delta_{kT}}{d}\left[\frac{3}{2}(0.2)^2 + \frac{3}{32}(0.2)^4 \cdots\right] \quad (16a)$$

where the factor Δ_{kT}/d occurs because we assume that the length of the flux bundle for which interactions must be accounted is equal to Δ_{kT} rather than the pin-

gests that cooperative flux motion dominates at fields above 7 T. That field varies almost linearly with pinning energy.

VII. SUMMARY

We have shown that magnetic flux lattice interactions are significant at fields above a few hundred gauss. These interactions interfere with thermally activated current-induced flux bundle hopping and reduce the superconductor's flux creep resistance below that estimated from the standard flux creep models which assume completely independent hopping.

ACKNOWLEDGMENTS

Discussions with Y. R. Lin-Liu and L. J. Campbell (Los Alamos National Laboratory) helped to clarify this exposition. This work was supported by the Department of the Navy, Office of Naval Research, under Contract No. N00014-88-C-7014.

REFERENCES

[1]A. M. Campbell and J. E. Evetts, Adv. Phys. **21**, 199 (1972).
[2]M. R. Beasley, R. Labusch, and W.W. Webb, Phys. Rev. **181**, 682 (1969).
[3]K. A. Müller, M. Takashige, and J. G. Bednorz, Phys. Rev. Lett. **58**, 1143 (1987).
[4]C. Rossel, Y. Maeno, and I. Morgenstern, Phys. Rev. Lett. **62**, 681 (1989).
[5]Y. Yeshurun and A. P. Malozemoff, Phys. Rev. Lett. **60**, 2202 (1988).
[6]M. Tinkham, *Introduction to Superconductivity* (McGraw Hill, New York, 1975), p. 141.
[7]M. Tinkham, *Introduction to Superconductivity* (McGraw-Hill, New York, 1975), p. 149.
[8]T.T. M. Palstra, B. Batlogg, L. F. Schneemeyer, and J.V. Waszczak, Phys. Rev. Lett. **61**, 1662 (1989); R. Griessen, C. F. J. Flipse, C.W. Hagen, J. Lensink, B. Dam, and G. M. Stollman, J. Less-Common Metals **151**, 39 (1989).
[9]M. Tinkham, *Introduction to Superconductivity* (McGraw-Hill, New York, 1975), p. 151.
[10]I. S. Gradshteyn and I. M. Ryzhik, *Table of Integrals and Products*, 4th ed. (Academic Press, New York, 1965), p. 26.
[11]*Handbook of Mathematical Functions*, edited by M. Abramowitz and I. A. Stegun (Dover Pub. Inc., New York, 1964), p. 379, Eq. 9.8.5.
[12]A large range of values have been measured, from 20 meV on up. See, for example, Y. Yeshurun, A. P. Malozemoff, and F. Holtzberg, 4th Joint MMM-Int. Conf. Vancouver, July 12–15, 1988 (U = 20 meV); R. Griessen, C. F. J. Flipse, C.W. Hagen, J. Lensink, B. Dam, and G. M. Stollman, "Critical currents and magnetic relaxation of epitaxial $YBa_2Cu_3O_{7-\delta}$ films," Proc. E-MRS Fall meeting, Strasbourg (France) and J. Less-Common Metals (1989) (U = 25 meV); C.W. Hagen and R. Griessen, a review article in *Studies of High Temperature Superconductors*, edited by A.V. Narlikar (Nova Science Publishers, Commack, New York, 1989), Vol. 3, pp. 159–195 (U = distribution peaked near 50 meV); T.T. M. Palstra, Critical Current Conference, Snowmass (CO) 1988; and T.T. M. Palstra, B. Batlogg, L. F. Schneemeyer, and J.V. Waszczak, Phys. Rev. Lett. **61**, 1662 (1988) (U > 400 meV).
[13]G. J. Dolan, G.V. Chandrashekhar, T. R. Dinger, C. Feild, and F. Holtzberg, Phys. Rev. Lett. **62**, 827 (1989).

Flux pinning in $Y_{1-x}Pr_xBa_2Cu_3O_{7-\delta}$ high T_c superconductors

L. M. Paulius, P. K. Tsai, J. J. Neumeier,[a] and M. B. Maple
Department of Physics and Institute for Pure and Applied Physical Sciences, University of California, San Diego, La Jolla, California 92093

K. C. Chen and K. S. Mazdiyasni
General Atomics, San Diego, California 92121

(Received 2 January 1991; accepted for publication 19 February 1991)

Magnetic relaxation measurements have been made on two sets of samples of $Y_{1-x}Pr_xBa_2Cu_3O_{7-\delta}$ high T_c superconductors with $0 \leqslant x \leqslant 0.10$. The samples were prepared as fibers using a sol-gel process and as polycrystalline pellets using a standard solid-state reaction technique. In an applied field of 5 kOe at 30 K, the fluxoid pinning potential U was observed to increase approximately linearly with Pr concentration x at the rate $dU/dx \approx 1$ eV. A mechanism for the enhancement of U may be the suppression of the superconducting order parameter in the vicinity of the Pr ions due to magnetic pair breaking.

Practical applications of superconductors require high critical current densities in the presence of high magnetic fields. Current densities in high T_c materials are limited by thermally activated flux motion due to low flux pinning energies and high temperatures. Intragranular critical current densities can be increased through the introduction of localized defects which act as fluxoid pinning centers.

Fluxoid pinning in a superconductor occurs at regions where the superconducting order parameter is suppressed. These regions may occur at structural defects or localized regions of different chemical composition. Structural defects in high T_c oxide superconductors have been introduced through ion,[1] neutron,[2] and electron[3] irradiation, as well as shock compaction.[4,5] The introduction of pinning centers through chemical doping, discussed below, has advantages in that it is nondestructive, offers better control of the impurity concentrations, and can be incorporated into a processing routine with minimal alteration.

In a number of studies, chemical doping resulting in the formation of nonsuperconducting phases has been shown to increase intragranular critical currents. Shi *et al.*[6] prepared a series of Bi-Sr-Ca-Cu-O samples with various starting concentrations of Ca and Cu. Intragranular critical current densities J_c deduced from magnetic hysteresis measurements increased with the amounts of Ca and Cu-rich precipitates. Increases in J_c were also found when $YBa_2Cu_3O_{7-\delta}$ and $LaBa_2Cu_3O_{-\delta}$ were prepared with Ca_2CuO_3 and $CaCu_2O_3$ by Mizuno *et al.*[7] Finally, magnetic measurements by Murakami *et al.*[8] showed increases in J_c and pinning energies when $YBa_2Cu_3O_{-\delta}$ was subjected to a special melt process resulting in finely dispersed inclusions of Y_2BaCuO_5.

The superconducting properties of $YBa_2Cu_3O_{-\delta}$ and $Y_{0.8}R_{0.2}Ba_2Cu_3O_{7-\delta}$ were reported recently by Jin *et al.*,[9] where all the rare-earth elements R were investigated with the exception of radioactive Pm. At a temperature of 77 K and an applied field of 0.9 T, enhancement of the intragranular critical current densities was observed in several samples, up to a factor of ~ 2.4 for R = Sm, Eu, and Gd.

Praseodymium is the only rare-earth element which forms the orthorhombic crystal structure $RBa_2Cu_3O_{-\delta}$ (where R is any rare-earth element with the exception of Ce, Tb, or Pm) but does not yield superconductivity.[10] Neutron diffraction studies[11] have shown that Pr substitutes for Y in $Y_{1-x}Pr_xBa_2Cu_3O_{7-\delta}$. The depression of T_c is slight for Pr concentrations $0 \leqslant x \leqslant 0.1$ ($T_c = 88$ K for $x = 0.1$ vs $T_c = 92$ K for $x = 0$). As the Pr concentration increases, the superconducting critical temperature T_c decreases monotonically, with superconductivity vanishing completely at $x \approx 0.56$. Thus, in the range $0 \leqslant x \leqslant 0.1$, the substitution of Pr for Y could introduce flux pinning centers separated by distances on the order of a lattice constant without significantly degrading superconductivity.

In this letter, we report the effects of chemical doping on flux pinning in the high-temperature superconductor $Y_{1-x}Pr_xBa_2Cu_3O_{7-\delta}$. Magnetic relaxation measurements are presented for two series of samples, prepared using different techniques, with Pr concentrations $0 \leqslant x \leqslant 0.1$. In an applied field of 5 kOe at 30 K, these results reveal that the pinning energy U increases nearly linearly with the Pr concentration at the rate $dU/dx \approx 1$ eV. A mechanism for the enhancement of U may be the suppression of the superconducting order parameter in the vicinity of the Pr ions due to magnetic pairbreaking.

Samples of $Y_{1-x}Pr_xBa_2Cu_3O_{-\delta}$ with varying Pr dopant concentrations were prepared as fibers using a sol-gel process and as polycrystalline pellets using a solid-state reaction technique.[12] Magnetic relaxation measurements were performed on these samples in order to estimate the pinning energies.

The pellets prepared by solid-state reaction were subjected to eight cycles of firing in air at 930 °C, with intermediate grindings. The firing schedule consisted of five cycles, each with a duration of 24 h, followed by cycles with durations of two, four, and six days. After the final grinding, the sample was pressed into pellets which were annealed in O_2 for two days at 955–970 °C, cooled slowly at 1 °C/min to 450 °C, allowed to soak for 18 h, and cooled slowly to room temperature. Resistive transition widths $\Delta T_c \equiv T_{c9} - T_{c1}$, where T_{cn} is the temperature at which

[a] Present address: Sektion Physik, Universität München, Schellingstrasse 4, D-8000 München 40, Germany

 0003-6951/91/161792-03$02.00

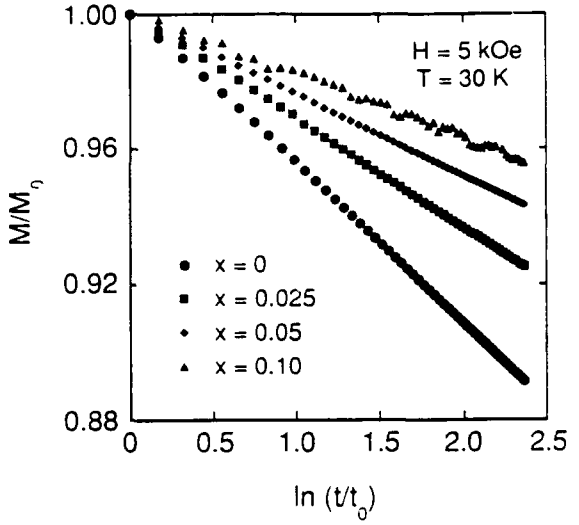

FIG. 1. Magnetic moment M of $Y_{1-x}Pr_xBa_2Cu_3O_{7-\delta}$ vs the natural log of the time t. Samples prepared by solid-state reaction with the indicated Pr concentrations were cooled in zero field to $T = 30$ K. Times are normalized to $t_0 \approx 95$ s after a magnetic field of 5 kG was applied. Moments are normalized to the values at t_0.

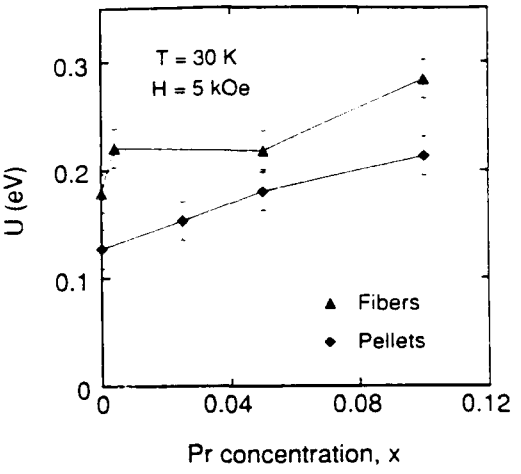

FIG. 2. Pinning energy U, deduced from the magnetic relaxation data, vs Pr concentration x for fibers prepared by the sol-gel process and pellets prepared by solid-state reaction. Error bars reflect the uncertainty in the hopping time.

the resistivity drops to a fraction n of its extrapolated normal state value, were less than 1 K. Iodometric titration revealed an oxygen content of 6.95 ± 0.02 (Ref. 12) for the samples. X-ray diffraction patterns showed the samples to be single phase.

Sol-gel fibers were prepared solutions containing isopropoxides of yttrium $Y(OC_3H_7)_3$, praseodymium $Pr(OC_3H_7)_3$, and barium $Ba(OC_3H_7)_2$, and copper ethylhexanoate $Cu(O_2C_8H_{15})_2$ in isopropanol, prepared as described in Ref. 13. A tractable resin precursor was prepared from a stoichiometric mixture of the starting solutions by controlled hydrolysis and drying. A viscous resin was produced by the subsequent addition of a mixture of polar and nonpolar solvents. Fibers of $Y_{1-x}Pr_xBa_2Cu_3O_{7-\delta}$ were drawn by mechanical spinning from the cohesive mass. The fibers were given identical heat treatments, with a maximum sintering temperature of 915 °C. The diameter of the fibers varied from 100 to 150 μm, and lengths of $\lesssim 1.5$ cm were used as samples. Electron micrographs revealed a typical grain size of ~ 1–2 μm. Superconducting transition temperatures, measured resistively, were comparable to those of samples prepared by solid-state reaction. Superconducting transition widths ΔT_c varied from in the range of 1.5 K to 3 K.

Magnetic relaxation data were obtained by cooling the samples in zero field and subsequently applying a magnetic field. The magnetic moment of each sample was recorded at regular time intervals after initial transients died down. In Fig. 1, magnetic relaxation data are shown for the pellets prepared by solid-state reaction, with $x = 0$, 0.025, 0.05, and 0.10. These data, taken at a temperature of 30 K and an applied field of 5 kOe, were recorded at intervals of ~ 48 s beginning at $t_0 \approx 95$ s.

The logarithmic time dependence of the magnetization can be related to a thermally activated movement of flux lines through the sample.[14] As discussed in Ref. 15, if a single barrier height for the pinning centers is assumed, the magnetic moment $M(t,T)$ can be calculated as[16,17]

$$M(t,T) = M_0(T)[1 - (kT/U)\ln(t/\tau)], \quad (1)$$

where $M_0(T)$ is the moment at time $t = 0$. $U = U(T)$ is the pinning energy, and τ is the hopping time ($10^{-12} < \tau < 10^{-6}$ s). Thus, the magnetization at a particular time t_0 is

$$M(t_0,T) = M_0(T)[1 - (kT/U)\ln(t_0/\tau)], \quad (2)$$

which can be used to eliminate $M_0(T)$ from Eq. (1). A plot of the normalized magnetization, $M(t,T)/M(t_0,T)$, as a function of $\ln t$ has a slope S_n given by

$$S_n = [U/kT - \ln(t_0/\tau)]^{-1}, \quad (3)$$

from which the pinning energy U can be calculated.

The magnetic relaxation data shown in Fig. 1 for samples prepared by solid-state reaction indicate that flux pinning increases with increasing Pr concentration under the conditions $H = 5$ kOe and $T = 30$ K. Values of U calculated from the slopes, plotted as diamonds in Fig. 2, indicate that the pinning energy increases almost linearly from a value of 0.13 eV in the undoped pellet to 0.21 eV in the $x = 0.10$ pellet. Error bars reflect the uncertainty in τ.

Magnetic relaxation measurements were also performed on fibers of $Y_{1-x}Pr_xBa_2Cu_3O_{7-\delta}$ prepared through the sol-gel process, with $x = 0$, 0.0036, 0.05, and 0.10. After cooling the samples to $T = 30$ K in zero field and applying a magnetic field of 5 kOe, the magnetic moment was measured every 57 ± 1 s beginning at $t_0 = 290$ s. Values of U, plotted as triangles in Fig. 2, show an increase in the pinning energy from 0.18 eV in the undoped fibers to 0.28 eV in the fibers with $x = 0.10$. The fibers with $x = 0.0036$ were crushed and remeasured; the pinning potential for the resulting powder was approximately 20% lower than for the fibers, indicating that some of the flux pinning probably occurs at the grain boundaries.

The increase in the pinning energies U with Pr doping were comparable in the pellets and fibers. From the undoped samples to the $x = 0.10$ samples, U increased by

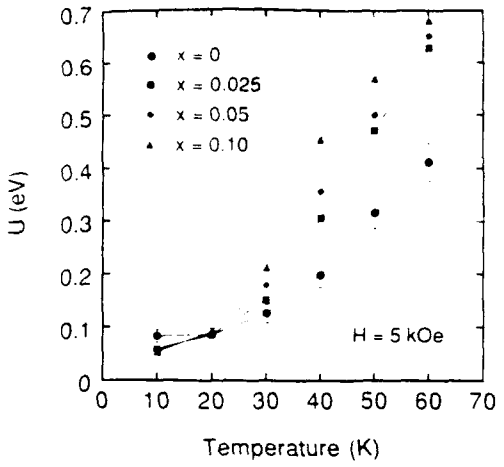

FIG. 3. Pinning energy U vs temperature at an applied field of 5 kG for samples prepared by solid-state reaction with indicated Pr concentrations x.

~ 0.1 eV, or $\gtrsim 60\%$. The values of U are higher for the fibers than for the pellets by ~ 0.05 eV. This may be related to the smaller grain size of sol-gel materials leading to an increased presence of grain boundaries which can act as pinning sites. Variations in the sample geometries and measurement times may also account for some of the differences between the pellet and fiber data.

For the samples prepared by solid-state reaction, pinning energies were determined over a range of temperatures from 10 to 70 K. In Fig. 3, pinning energies calculated using Eq. (3) are plotted as a function of temperature for the series of Pr concentrations. The data indicate that the pinning energy increases as a function of Pr concentration at temperatures > 20 K.

The increase of the flux pinning potential U upon substitution of Pr for Y in $YBa_2Cu_3O_{7-\delta}$ is presumably due to the suppression of the superconducting order parameter in the vicinity of the Pr ions. A mechanism for this effect may be superconducting electron pair breaking via spin dependent exchange scattering of holes in the conducting CuO_2 planes by the Pr ions. The combined effects of superconducting electron pair breaking and hole filling (or localization) have been invoked to account for the variation of T_c with x and applied pressure in the $Y_{1-x}Pr_xBa_2Cu_3O_{7-\delta}$ system, based upon an analysis of measurements of $T_c(x,y)$ on the $Y_{1-x-y}Pr_xCa_yBa_2Cu_3O_{7-\delta}$ system.[18] Hybridization of the Pr $4f$ localized states and the CuO_2 valence band states could provide a mechanism for the filling (or localization) of holes in the CuO_2 planes and generate an antiferromagnetic exchange interaction between the Pr magnetic moments and the spins of the mobile holes in the CuO_2 planes via the Schrieffer–Wolf transformation.[10,18]

Further work is in progress on the samples prepared by solid-state reaction. Intragranular critical current densities will be determined magnetically. The measurement range will be extended to other applied fields and to samples with Pr concentrations $0.10 < x \leq 0.6$. Measurements on single crystals of $Y_{1-x}Pr_xBa_2Cu_3O_{7-\delta}$ will elucidate the role of grain and twin boundaries and enable us to investigate flux pinning anisotropy.

We acknowledge enlightening discussions with C. C. Almasan. Work at General Atomics was supported by DARPA/ONR contract No. N00014-88-C-0714. Work at UCSD was supported by a subcontract from DARPA/ONR contract No. N00014-88-C-0714 and by US DOE contract No. DE-FG03-86ER45230.

[1] B. Roas, B. Hensel, G. Saemann-Ischenko, and L. Schultz, Appl. Phys. Lett. **54**, 1051 (1989).
[2] H. Kupfer, I. Apfelstedt, W. Schauer, R. Flukiger, R. Meier-Hirmer, H. Wuhl, and H. Scheuer, Z. Phys. B **69**, 167 (1987).
[3] Y. Matsui, E. Takayama-Muromachi, and K. Kato, Jpn. J. Appl. Phys. **26**, L1183 (1987).
[4] C. L. Seaman, E. A. Early, M. B. Maple, W. J. Nellis, J. B. Holt, M. Kamegai, and G. S. Smith, in *Shock Compression of Condensed Matter-1989*, edited by S. C. Schmidt, J. N. Johnson, L. W. Davison (North Holland, New York, 1990), pp. 571–574.
[5] S. T. Weir, W. J. Nellis, M. J. Kramer, C. L. Seaman, E. A. Early, and M. B. Maple, Appl. Phys. Lett. **56**, 2042 (1990).
[6] D. Shi, M. S. Boley, U. Welp, J. G. Chen, and Y. Liao, Phys. Rev. B **40**, 5255 (1989).
[7] F. Mizuno, H. Masuda, I. Hirabayashi, and S. Tanaka, in *High-Temperature Superconductors: Fundamental Properties and Novel Materials Processing*, edited by J. Narayan, C. W. Chu, L. F. Schneemeyer, and D. K. Christen (Materials Research Society, Pittsburgh, PA, 1990), pp. 955–958.
[8] M. Murakami, S. Gotoh, H. Fujimoto, N. Koshizuka, and S. Tanaka, presented at the Conference on Materials Science and Application of High Temperature Superconductors, Greenbelt, MD, 1990.
[9] S. Jin, T. H. Tiefel, G. W. Kamlott, R. A. Fastnacht, and J. E. Graebner, Physica C **173**, 75 (1991).
[10] M. B. Maple, J. M. Ferreira, R. R. Hake, B. W. Lee, J. J. Neumeier, C. L. Seaman, K. N. Yang, and H. Zhou, J. Less-Common Met. **149**, 405 (1989), and references cited therein.
[11] J. J. Neumeier, T. Bjørnholm, M. B. Maple, J. J. Rhyne, and J. A. Gotaas, Physica C **166**, 191 (1990).
[12] K. C. Chen, A. Y. Chen, and K. S. Mazdiyasni, *Better Ceramics Through Chemistry IV*, edited by B. J. J. Zelinsky, C. J. Brinker, D. E. Clark, and D. R. Ulrich (Materials Research Society, Pittsburgh, PA, 1990), pp. 913–916.
[13] K. C. Chen and K. S. Mazdiyasni, in *High-Temperature Superconductors: Fundamental Properties and Novel Materials Processing*, edited by J. Narayan, C. W. Chu, L. F. Schneemeyer, and D. K. Christen (Materials Research Society, Pittsburgh, PA, 1991), pp. 1213–1216.
[14] P. W. Anderson, Phys. Rev. Lett. **9**, 309 (1962).
[15] C. C. Almasan, C. L. Seaman, Y. Dalichaouch, and M. B. Maple, Physica C **174**, 93 (1991).
[16] C. W. Hagen, R. P. Griessen, and E. Salomons, Physica C **157**, 199 (1989).
[17] M. Tinkham and C. J. Lobb, in *Solid State Physics 42*, edited by H. Ehrenreich and D. Turnbull (Academic, New York, 1989), pp. 91–134.
[18] M. B. Maple, N. Y. Ayoub, J. Beille, T. Bjørnholm, Y. Dalichaouch, E. A. Early, S. Ghamaty, B. W. Lee, J. T. Markert, J. J. Neumeier, G. Nieva, L. M. Paulius, I. K. Schuller, C. L. Seaman, and P. K. Tsai, in *Transport Properties of Superconductors*, edited by R. Nicolsky (World Scientific, New York, 1990), pp. 536–556, and references cited therein.

Solution Condensed $YBa_2Cu_3O_{7-x}$ Superconductor Thin Films from Thermosetting Metal-Organic Precursors

S. S. Pak*, F. C. Montgomery, D. M. Duggan, K. C. Chen*, and K. S. Mazdiyasni*

General Atomics, San Diego, 92186-9784

P. K. Tsai, L. M. Paulus and M. B. Maple

University of California at San Diego, La Jolla, 92093

ABSTRACT

Two different multimetal organic compounds were synthesized and used to deposit thin Y:Ba:Cu oxide films on selected metal and ceramic substrates by dip coating method. The rheology of the precursors are strongly influenced by the organic ligand, types of solvent, solvent-water molar ratio and processing method. The precursor compounds were converted to suitable viscosity for uniform thickness film processing on complex geometry. Superconducting transition temperature T_c in the range of 89 to 93 K have been measured depending on processing parameters used. The critical current density, J_c of the solution coated films were not as high as expected due to the high temperature processing and chemical reaction with the substrates. Y123 film exhibit c-axis alignment on Ag substrate. Prototype high Q cavity was coated with Y123 and its performance was evaluated. (Key words: high temperature superconductors, solution coating, complex geometry, multimetal organic precursors.)

---

* Members of the American Ceramic Society

I. INTRODUCTION

Following the discovery of $YBa_2Cu_3O_{7-x}$[1] and the related family of superconductors[2,3] intensive effort has been made to fabricate the new superconductors into useful electronic devices, such as SQUIDs (Superconducting Quantum Interference Devices), resonators, A/D converters, band pass filters and ultimately, supercomputers. Needless to say that all these applications require uniform thickness superconductor in thin film form on nonreactive substrate of low dielectric constant and loss tangent with matching coefficient of thermal expansion. Recent reports of high quality $RBa_2Cu_3O_{7-x}$ (R = rare earth) films grown on sapphire and $LaAlO_3$ by physical vapor deposition processes (such as laser ablation, sputtering, and electron beam evaporation) have brought much promise and optimism[4,5]. Despite the promising reports, physical vapor deposition processes are not suitable for large-scale components production and/or complex shape devices, because of their inherent high vacuum requirement and line-of-sight deposition method.

The sol-gel/dip and or spin-on coating techniques have been shown to be very effective in depositing highly uniform and pure complex oxides at low temperatures in addition to having the advantage of overcoming the aforementioned limitations.[6,7] However, despite its easy application, the high T_c films processed by the sol-gel method have not yet measured up in quality with those produced by physical vapor deposition techniques. The causes for the poor film quality are attributed to the inhomogeneities rendered by (1) the low solubility of Cu compounds

in common organic solvents, which prevents mixing of the constituent at the molecular level; (2) vastly different polycondensation rates among constituent metals, which causes chemical segregation; and (3) the unfavorable thermodynamic and sluggish reaction kinetics to form phase pure superconductor[8-10] below 700°C which makes high processing temperature and thereby higher reactivity with the substrate unavoidable. Thus, almost all of the sol-gel methods of fabricating $YBa_2Cu_3O_{7-x}$ (YBCO) films reported in the literature[11-27] have invariably focused on overcoming these issues.

The purpose of this paper is to highlight the chemical pathways, physical and rheological property requirements of the ceramic precursor, which must be controlled and are essential in developing the YBCO solution condensed thin film on metals and ceramic substrates.

For the purpose indicated, the sol must be thermosetting, in addition to being mutually soluble in a common solvent and its constituent metals being polymerizable at a similar rate. The thermosetting quality is highly important in maintaining film uniformity. In contrast, a thermoplastic coating would run and sag during drying and curing. Most of the sol-gel methods reported in the literature neglect this very important quality. Also the development of a thermosetting sol, which allows the deposition of thin $YBa_2Cu_3O_{7-x}$ films on complex geometry is stressed. Ag and yttria-stabilized zirconia polycrystal (YSZP), Zyttrite®, and $SrTiO_3$ were chosen as the substrate materials for either their low loss factor and/or thermal expansion match, and relative

chemical inertness.[28,29] It will be shown that c-axis alignment was achieved by a proper heat treatment schedule. Most importantly, the processing method described allows large, difficult to coat surface geometries to be coated with $YBa_2Cu_3O_{7-x}$.

II. EXPERIMENTAL PROCEDURE

Synthesis of Precursor Compounds

Two different types of metalorganics, metal alkoxides plus a metal organic salt and mixed ligand alkoxides were used to develop 123 films on different substrates.

1. *Metal Alkoxides and Copper Organic Salt Method*

Yttrium isopropoxide, $Y(OC_3H_7)_3$ and barium isopropoxide, $Ba(OC_3H_7)_2$, were synthesized by the reaction of their respective metal chips* with excess anhydrous isopropanol.[30-32] Copper ethyl hexanoate solution was prepared by dissolving commercially available crystalline $Cu(O_2C_8H_{15})_2$** in anhydrous isopropanol. The three stock solutions were then mixed to form $YBa_2Cu_3O_{7-x}$ stoichiometry as shown in the flow diagram, Fig. 1.

Green precipitates formed soon after mixing. This suspension was brought into solution by refluxing for 2 hr under dry N_2 and subsequently adding 10 equivalents of water per mole of yttrium, while

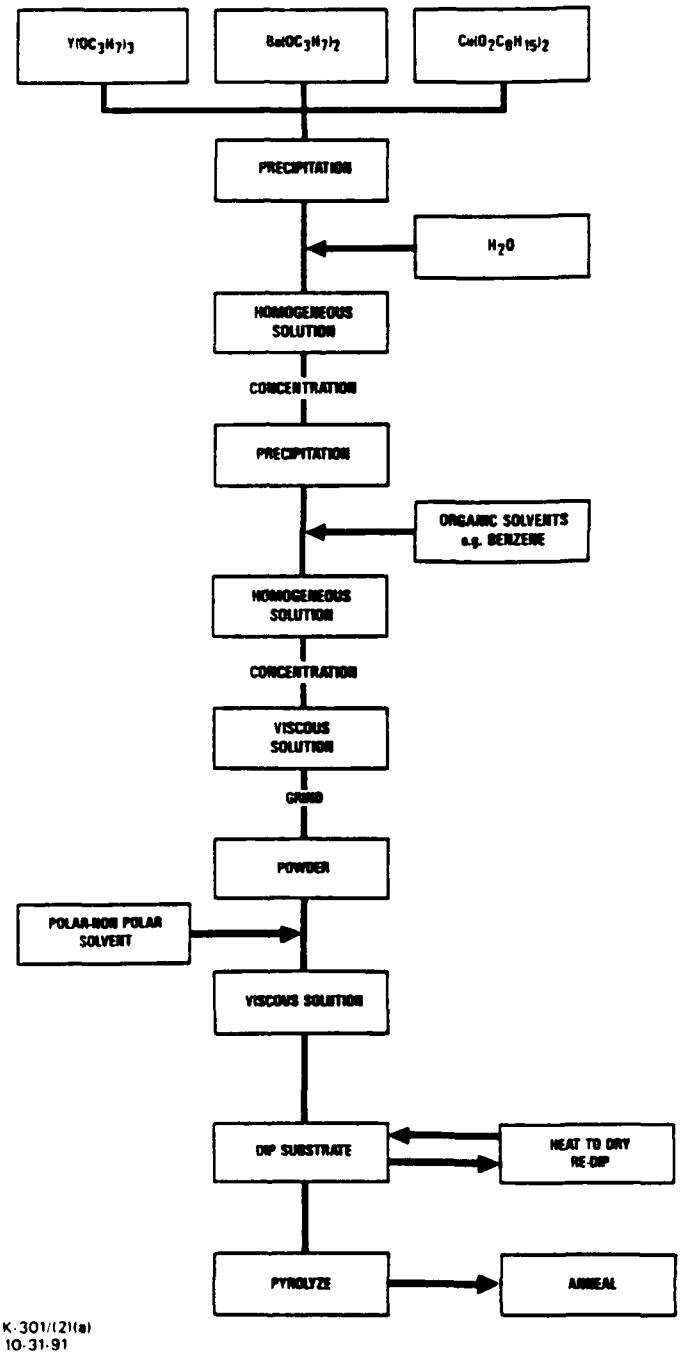

Fig. 1. Process flow for metal alkoxides, copper organic salt method

stirring. The stable, clear and homogeneous green solution was then rotary evaporated, further dried in a vacuum oven, and ground to a dry "resin" like powder and stored for thin film application. This dry "resin" readily re-dissolves in various binary polar and nonpolar solvents.

2. Mixed-ligand Alkoxides Method

Homogeneous solutions were also prepared using $Y(OR)_3$, $Ba(OR)_2$, and the copper (II) mixed-ligand species $(C_3H_7O_2)_2Cu_2(\mu\text{-}OR)_2$, where R = $CH_2CH_2OCH_2CH_2OCH_2CH_3$ and $C_5H_7O_2$ = 2,4-pentanedionate[33] shown in the flow diagram Fig. 2.

Yttrium tris-2-(2-ethoxyethoxy)ethoxide was prepared by alcohol exchange of yttrium isopropxide with anhydrous 2-(2-ethoxyethoxy)ethanol. In an oven dried 125 ml Erlenmeyer flask was added ' g yttrium isopropoxide and 10 ml dry 2-(2-ethoxyethoxy)ethanol. The flask was fitted with a drying tube and a N_2 inlet. The mixture was heated at 100° to 120°C until all the isopropoxide had dissolved. Heating was continued for 6 hr under a N_2 purge to remove isopropyl alcohol as it was formed. After cooling, the solution was centrifuged and decanted to remove a small amount of residue. A clear, pale yellow solution resulted. Ethylene diamine tetra acidic acid (EDTA) volumetric titration of the yttrium content verified the concentration and showed that the solution was stable for several weeks.

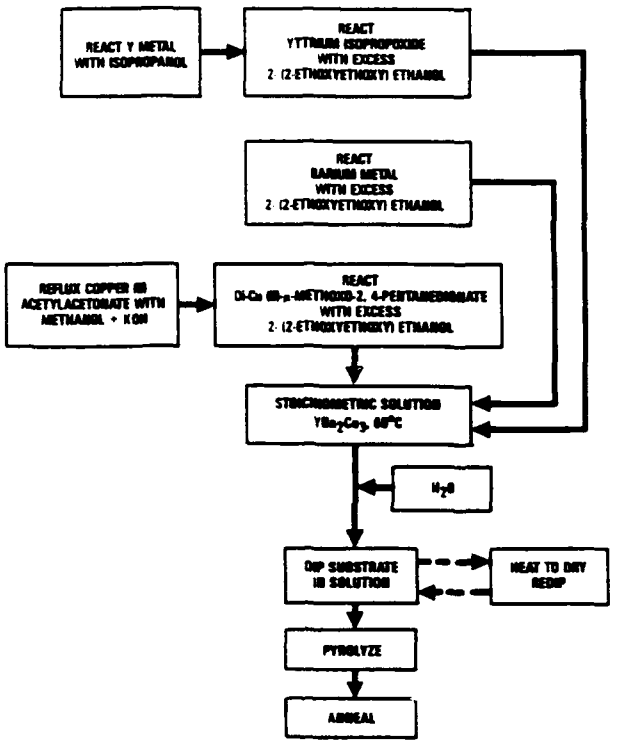

Fig. 2. Process flow for Cu(II) mixed-ligand method

The copper compound was synthesized by reaction of Di-Cu(II)-μ-methoxy-2,4-pentanedionate with anhydrous 2-(2-ethoxyethoxy)ethanol following a similar procedure used for the preparation of the yttrium compound. EDTA volumetric titration again indicated that the solution was stable for several weeks.

Barium 2-(2-ethoxyethoxy)ethoxide was prepared by reaction of barium metal granules (Alfa inorganics) with dry 2-(2-ethoxyethoxy)-ethanol. Typically, 3.96 g of barium was reacted with about 30 ml of dry alcohol. After the reaction was complete, as evidenced by the cessation of hydrogen evolution, the solution was filtered to remove a small amount of residue.

Hydrolysis (using less than two moles of water per mole of metal) was accomplished by injecting a dilute solution of the required amount of water in 2-(2-ethoxyethoxy)ethanol into the alkoxide solution. The thermal conversion of both of these metal organic precursors, resulted in very smooth surface finish, 99.95%, orthorohmbic single phase (high purity thin film on metal as well as ceramic substrates.

The chemical composition was determined by wet chemistry and minor impurities were analyzed by emission spectroscopy. The phase purity was determined by XRD.

The ratio of the constituents were adjusted until no low melting phases, other than the endothermic peak corresponding to the latent heat of melting for YBCO at 1043.75°C, was detected in DTA Fig. 3.

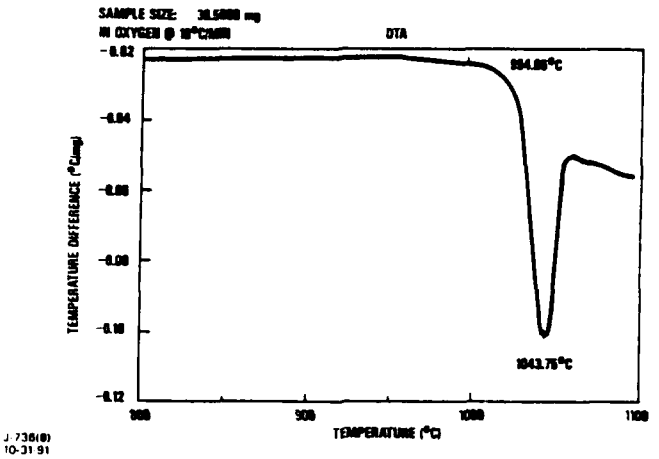

Fig. 3. DTA of the powdered 123 film sample with no evidence of low melting phase

Yttria-stabilized zirconia polycrystal (YSZP) and $SrTiO_3$ single crystal[+] substrate were cut to dimensions of approximately 3 x 15 x 0.1 mm. Each subtrate was ultrasonically cleaned in a dilute HNO_3 bath, rinsed with distilled water and then with isopropanol, and finally by holding them above boiling isopropanol. Thin film deposition was accomplished by dipping the substrates in the sol, pulling at 3 mm/min, and curing in nitrogen, oxygen, or air at a temperature between 500° and 700°C. The process was controlled by an automatic bench-top dip coater shown in Fig. 4. The process was repeated until a coating with the desired thickness was developed. Depending on solution concentration, typically, five to seven cycles had to be performed to build up a layer of 0.5 to 1 μm in thickness. The films were heated in a silver crucible in a microbalance equipped with alumina muffle tube or in alumina tube furnace to a temperature between 825° and 920°C in flowing oxygen, held from 1 min to 3 hr, cooled to 400° or 500°C at 2°C/min and hold up to 24 hr. Four silver pads were then sputtered along the length of the substrate using an aluminum mask, whose windows were approximately 1 mm x 3 mm. The outer two current pads were spaced 1 mm from the two inner voltage pads, which were 4 mm part. Thus, about 12 mm^2 of the film was tested. Electrical contacts were made by applying silver paste[+] between silver wires and pads. Electrical resistance was measured by the DC four point probe method using a Liner Research LR-400 Four Wire ac Resistance Bridge, with a current of 0.1 μA at 13 Hz. DC magnetic susceptibility was measured on a Quantum Design MPMS SQUID susceptometer. The measurement was conducted, while cooling the samples in zero magnetic field to 5 K, turning on a field of 30 Oe, heating to 120 K, and finally cooling to 5 K

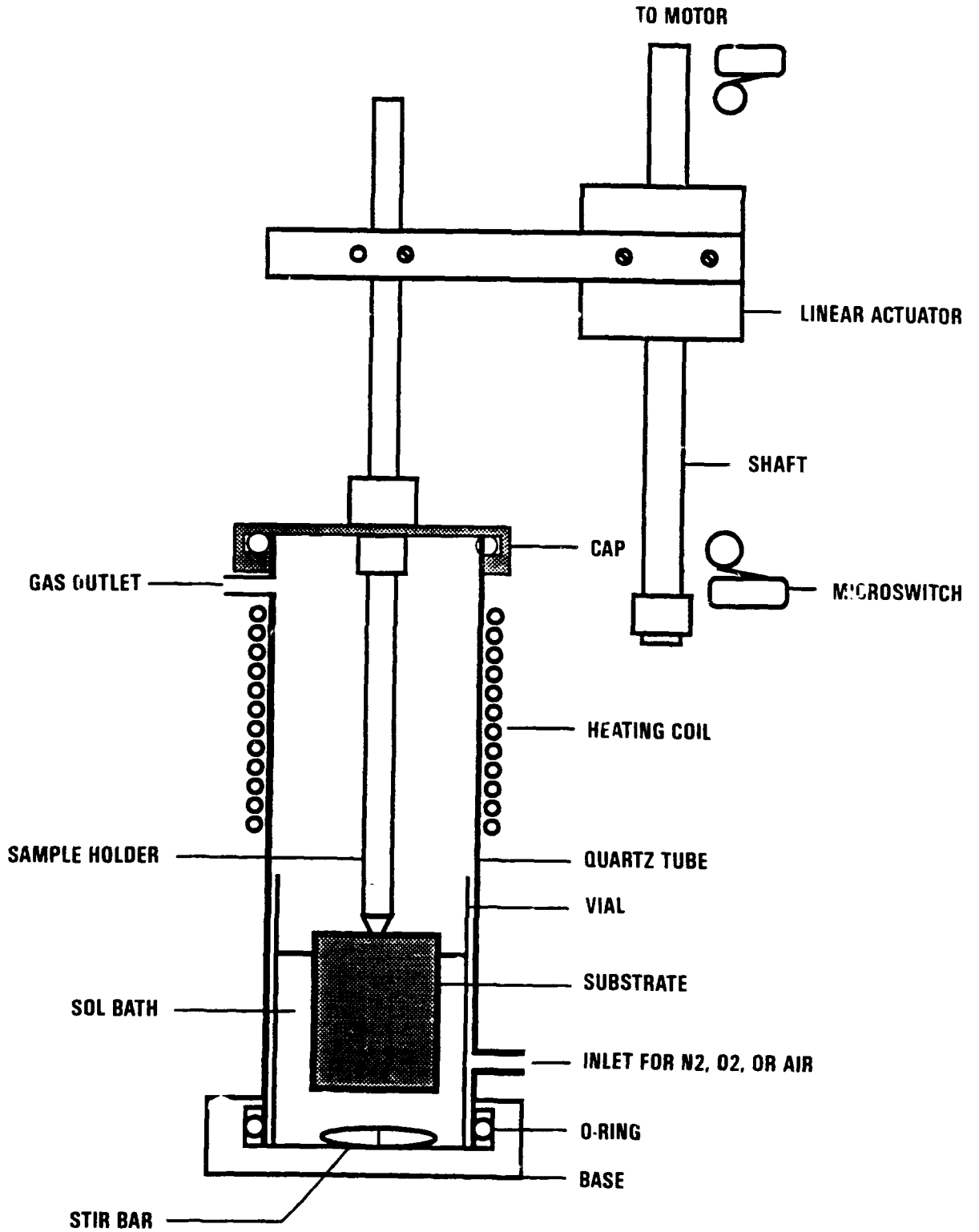

Fig. 4. Bench top automatic dip coater

Also the components of a prototype high Q cavity were coated with a thin film of 123. A silver cylinder of 0.5 in. diameter and 1 in. length was machined, polished, and cleaned with isopropanol prior to dipping. A matching pair of 0.5 in. diameter discs were also machined, cleaned, and polished. All three pieces were dipped four times and heated to 920°C in flowing oxygen, held for 30 min and furnace cooled until 400°C, at which point an isothermal soak of 8 hr was performed. Its surface resisitivity and the quality factor, Q, were measured as a function of temperature.

*Alfa Products, Ward, MA
**Aldrich, Milwaukee, WI
+Ted Pella, Inc., Redding, CA
++Superconductive Components, OH

III. RESULTS AND DISCUSSION

The rheology of metal alkoxide-copper organic salt and mixed-ligand alkoxides are strongly influenced by the presence of different kinds of solvents as well as their relative amounts. Noticeable viscosity changes were observed with small quantity of polar and non-polar solvent ratios. Under optimum condition, eq. 30 wt % precursor compound and 1:4 solvent ratio such as i-prOH and toluene the resin like precursor was converted to suitable viscosity for film processing. Also the Y:Ba:Cu stoichiometry as well as molar ratio of water to precursor compound have a marked effect on solution homogeneity and rheology for thin film deposition.

1. 123 FILM ON YSZP "ZYTTRITE®"

In order to determine the stoichiometry, film thickness and processing effects on the electrical properties of superconducting films, solutions from the mixed ligand process listed in Table I were prepared in accordance with the described experimental procedures and dip coated onto Zyttrite®, yttria fully stabilized zirconia polycrystal (YSZP), substrates. Figure 5 shows the electrical resistivity of a typical film prepared with a mixed ligand alkoxide solution. It exhibits metallic behavior and has a transition temperature width of a few degrees K.

Zyttrite® is ultra-high purity yttria fully stabilized zirconia polycrystal.

TABLE I
EFFECT OF PROCESSING PARAMETERS ON THE ELECTRICAL PROPERTIES OF THIN FILMS PREPARED BY THE MIXED-LIGAND METHOD ON YSZP

ID	Composition (Y:Ba:Cu)	Thickness (μm)	Sintering Temperature[a] (±2°C)	O_2 Annealing Time at 404 (±2°C)	T_c (K)	ΔT (K)
1	1.03:2.00:3.00	0.4 ± 0.1	900	24 hr	89	14
2	1.03:2.00:3.00	1.5 ± 0.5	900	24 hr	91	6
3	1.03:2.00:3.00	1.5 ± 0.5	900	1 hr	91	7
4	1.03:2.00:3.00	1.5 ± 0.5	905	24 hr	91	5
5	1.03:2.00:3.00	1.5 ± 0.5	910	24 hr	91	6
6	1.03:2.00:3.00	1.5 ± 0.5	920	24 hr	91	7
	1.03:2.00:3.00	1.5 ± 0.5	920	24 hr	91	4
7	1.00:2.00:3.00	1.5 ± 0.5	905	24 hr	90	7
	1.00:2.00:3.00	1.5 ± 0.5	920	24 hr	93	16
8	1.03:2.00:3.17	1.5 ± 0.5	905	24 hr	90	8
9	1.03:2.00:3.17	1.5 ± 0.5	910	24 hr	91	4
10	1.03:2.00:2.99	1.5 ± 0.5	900	1 hr	91	4
11	1.03:2.00:2.99	1.5 ± 0.5	900	1 hr	91	7
12	1.03:2.00:2.99	1.5 ± 0.5	905	12 hr	92	8

[a] 10 min at temperature.

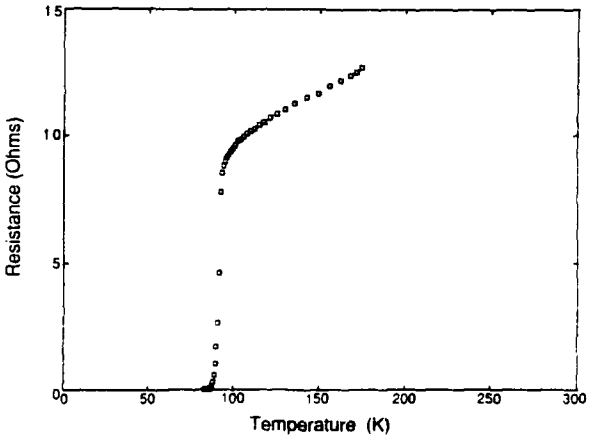

Fig. 5. Resistivity as a function of decreasing temperature for an $YBa_2Cu_3O7-\delta$ thin film on yttria-stabilized zirconia. The superconducting transition occurred with a midpoint at 91 K and a width of 4 K

The superconducting transition can be described by two parameters T_c and ΔT (T_c is the temperature of 50% of the value extrapolated from the normal state and the transition width, $\Delta T = T_{90} - T_{10}$, where T_{90} and T_{10} are 90% and 10%. Table I summarizes the processing conditions and the transition parameters for several films made by the mixed ligand method.

The first two results in Table I show that the thickness of the film affects the transition temperature. Based on the weight of material deposited, the thickness of the film produced by four dips is 1 to 2 μm. Thus, the film dipped once would be 0.25 to 0.5 μm thick. The thicker film results in a sharper transition from the normal to the superconducting state, and significantly lowers the initial resistance of the normal state. Currently, it is assumed that this is being caused by reaction of a certain volume of the film with the substrate. Similar results were seen with films prepared by the alkoxide plus copper organic salt method.

In investigations of thin film deposition by various techniques, the detrimental effects of superconductor-substrate interactions have been reported.[34] The reaction of 123 (Y:Ba:Cu) with ZrO_2 is known to occur at temperatures as low as 600° and at 945°C results in the formation of CuO, $BaZrO_3$ and the 211 compound.[35]

A preliminary observation indicating that reaction with YSZP substrate may be occurring during the processing of the sol-gel derived

films from a stoichiometric solution is shown in Fig. 6. The transition temperature in this film began at 93 K and had a ΔT of 16 K. The SEM shows the morophology of the film which has been processed at 921°C for 10 min and oxygen annealed at 404°C for 24 hr. Two distinct layers are evident in the film at the bottom of the substrate. EDAX analysis of top layer (Y:Ba:cu = 1.26:2.07:3.00) agreed with microprobe analysis (1.24:2.11:3.00) of specific areas on the surface of a film made from the same precursor solution. Microprobe analysis of the surface of the films indicates that the surface is not single phase 123. Instead, the films have areas with the correct stoichiometry interspersed with a phase that has the proper Ba:Cu ratio but is high in yttrium. In addition, there are some spots that are high in yttrium and depleted in copper. The lower layer seems to be enriched in copper indicating a loss of barium.

Also the stoichiometry of the solution, depicted in Table I, affects the sharpness of the superconducting transition of the film. The superconducting transitions for films prepared from the Y-rich solution (4) have sharper ΔT values than the film prepared from stoichiometric (7) and Cu-rich solution (8).

The homogeneity of the coatings formed on YSZP were found to depend on the conditions used during the hydrolysis of the initial reaction mixture. Solutions that were hydrolyzed with more than 2 moles of water per mole of metal precipitated barium and the coatings prepared from this solution were, thus, low in barium.

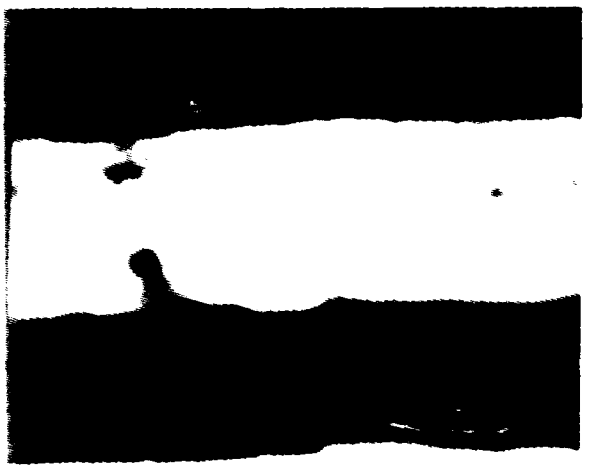

Fig. 6. SEM photograph showing morophology of superconducting film and apparent reaction layer

When the reaction conditions were such that either the extent or rate of hydrolysis was low or the viscosity of the solution did not change due to inadequate polymerization, the final coatings showed segregation of the individual constitutents, with copper being present as nodules of CuO. Figure 7 is an SEM photograph at a magnification of 4000X showing the microstructure of this type of coating and CuO nodule at the top of the picture.

Figure 8 shows a SEM photograph of a coating that was prepared from a solution containing about 17 wt % equivalent 123 compound and that had polymerized sufficiently to increase the solution viscosity. EDAX line measurements showed that the coating stoichiometry is homogeneous. Furthermore, the coating shown in Fig. 8 has less void than the coating shown in Fig. 7. Magnetic flux measurements showed that this coating exhibited a Meissner effect beginning around 90 K.

The coating heat treatment is also important in establishing the final microstructure of the coating. Significant amounts of grain growth were observed by increasing the firing temperature form 882° to 958°C coating shown in Fig. 8.

Increasing the processing temperature does not have a large effect on the superconducting properties of the film. The width of the transitions for films heat treated to 900°, 905°, 910°, and 920°C (±2°C) were similar. However, the resistance of the normal state at 100 K was higher for the 910°C processed film. The possible cause of variability

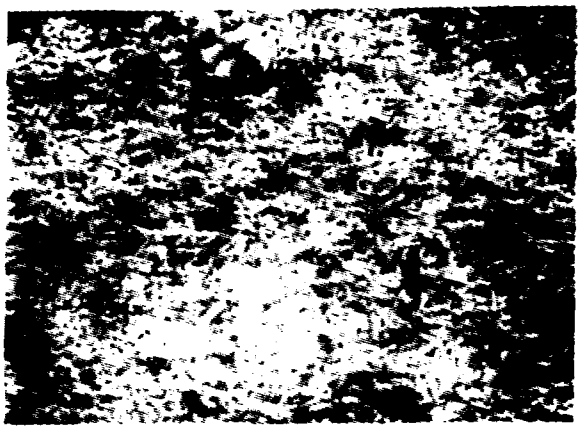

Fig. 7. SEM of Y123 thin film showing CuO nodules

Fig. 8. SEM of higher density Y123 film with no evidence of CuO nodules

of the high resistance of these films are speculated to be the chemical reaction and or diffusion of mobile ions such as Ba^{++} and Cu^{++} in the YBCO system. Diffusion barrier such as $BaZrO_3$ has been shown to improve the electromagnetic properties of thin films on various substrate materials.

The results in Table I shows that the transition temperature of films are not affected by the annealing time at 400°C. The samples that were cooled slowly between 500° and 403°C with only a 1 hr hold had the same properties as did the samples oxygenated for a longer time [samples (2) and (3)]. Thus a 24-hr oxygenation may not be required to obtain a sharp resistance drop at 92 K.

2. 123 Film on $SrTiO_3$

Thin films of Y123 were prepared by dipping single crystal $SrTiO_3$ in a sol of the alkoxide copper organic salts in toluene and i-PrOH as shown in flow diagram Fig. 1. The resin was approximately 30 wt % and the rest 70 wt % is a binary solvent consisting of toluene to i-PrOH in 4:1 ratio. The substrate was multiply dipped in air and pyrolyzed at 500°C in between each dip. Thus obtained film was fired at 825°C for 1 min in flowing O_2. The purpose of low temperature and short time firing as compared to the alkoxides mixed-ligand process was to minimize the chemical reaction between the substrate and the film. The film was fully oxygenated by holding at 400°C for 19 hr in flowing O_2 atmosphere.

As the resistance curve Fig. 9 shows, the film exhibited a metallic characteristic. The measured Tc was approximately 80 K and Jc = 400 A/cm^2 at 30 K at 0 field. The XRD pattern Fig. 10 shows the film is highly oriented with its c-axis perpendicular to the substrate surface.

3. 123 Film on Silver (Ag)

Because of its chemical inertness polycrystalline Ag was chosen as the substrate material. Since it is crucial to develop a highly dense and smooth film for most applications mentioned previously, it was necessary to determine the optimum heat treatment schedule for full densification and the attainment of fine grain size YBCO on Ag substrate. Figure 11 shows the microstructures of the $YBa_2Cu_3O_{7-x}$ films by alkoxide organic salt method on Ag substrate after heat treatment as function of times. The SEM show that full densification does not occur even at 920°C for 10 min. However, by holding at 920°C for 3 hr, full densification and plate-like morphology were developed. An x-ray diffraction pattern shown in Fig. 12, reveals that (001) peaks are enhanced when the films were heat treated beyond 920°C for 10 min. As observed in the SEM, the degree of c-axis alignment improved dramatically with increasing isothermal holding time. For example, the ratio of (006) to (110) peak was 12 for the sample heat treated 30 min at 920°C, whereas it was 200 for the sample held at the same temperature for 3 hr.

There were 0.1 to 0.4 μm wide (both intergranular and intragranular) cracks throughout the film as shown in Fig. 13. They are believed

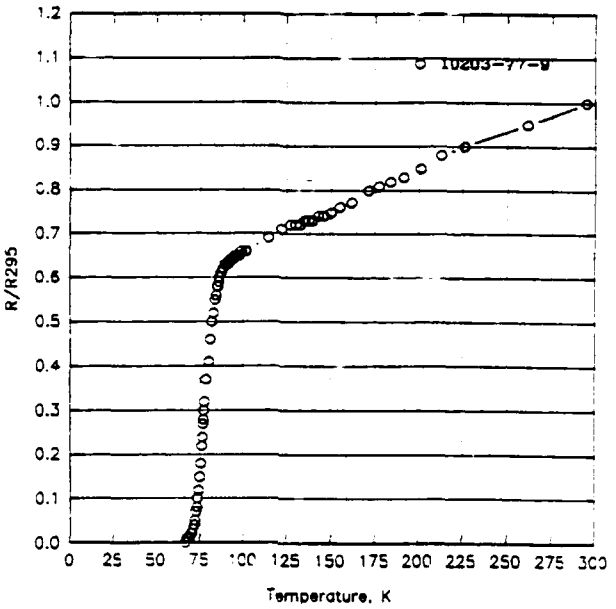

Fig. 9. Effect of film thickness on superconducting resistance

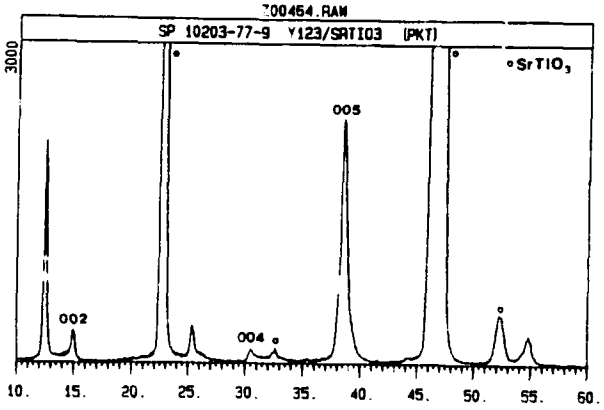

Fig. 10. XRD pattern of 123 on $SrTiO_3$

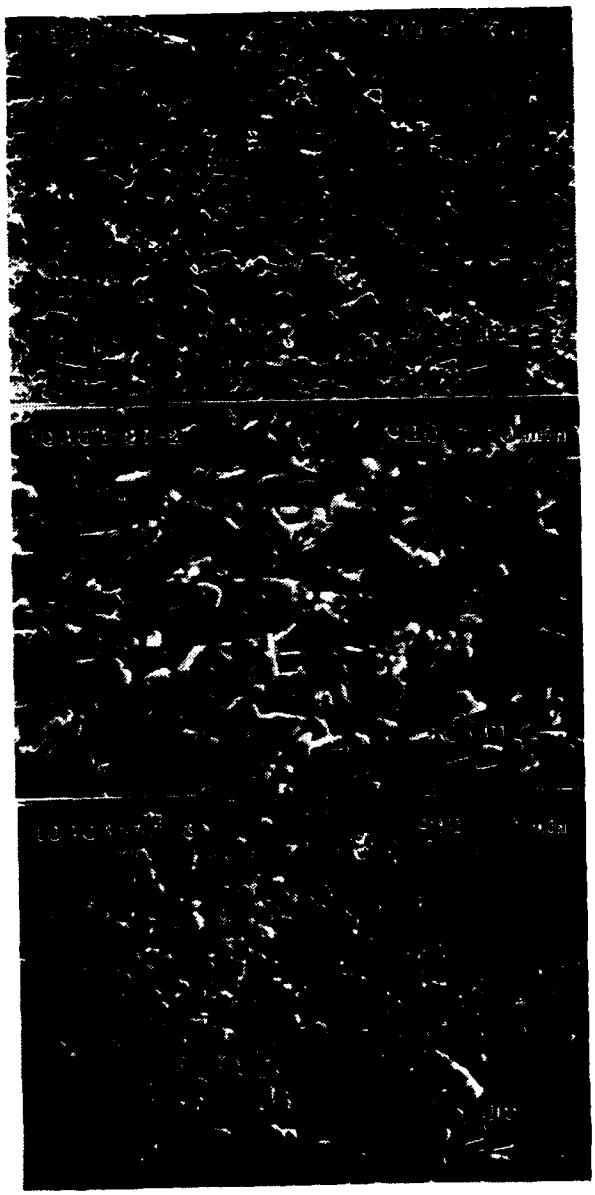

Fig. 11. SEM of 123 coated silver substrate heat treated at 920°C for different times

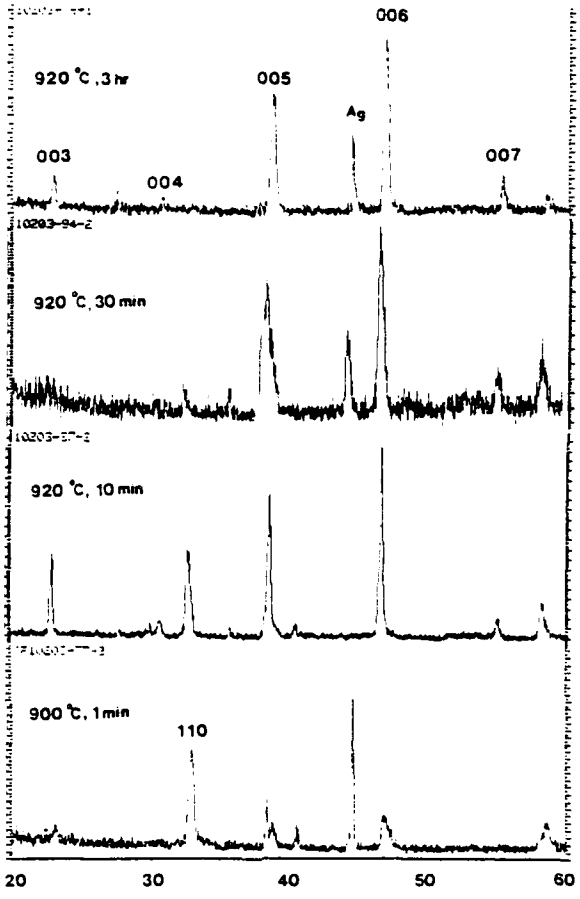

Fig. 12. X-ray diffraction patters as a function of time and temperature showing 123 C-axis orientation on silver substrate

Fig. 13. SEM of high density 123 film on silver substrate with numerous microcracks

to be caused by the lower thermal expansion coefficient of Ag (14 x 10^{-6}°C compared to 16.9 x 10^{-6}/°C for $YBa_2Cu_3O_{7-x}$) inducing tensile stress in the film during cooling.

Substrate Grain Size Effect on Grain Alignment

In order to test whether grain growth of Ag was responsible for c-axis alignment, a pair of Ag substrates were prepared. One was heat treated in O_2 at 920° for 10 min and the other was left untreated. The heat treatment caused the Ag grains to grow to size approximately 1 mm in diameter. The two substrates were dipped simultaneously and heat treated at 920°C for 30 min in flowing O_2.

The XRD results Fig. 14 show the film on heat treated Ag was aligned twice as much by peak intensity as the one without the heat treatment. This clearly shows a heteroepitaxial growth mechanism for the 123 grain alignment on silver. The exact orientation relationship between the substrate and the film is yet to be elucidated.

Since it was difficult to measure the quality of the film on Ag by dc resistance, due to the exceptionally low resistivity of Ag making the data above T_c suspect, a dc susceptibility measurement was carried out instead. The summary of the electromagnetic properties of the films deposited on YSZP, $SrTiO_3$, and Ag by the two different chemical pathways are shown in Table II.

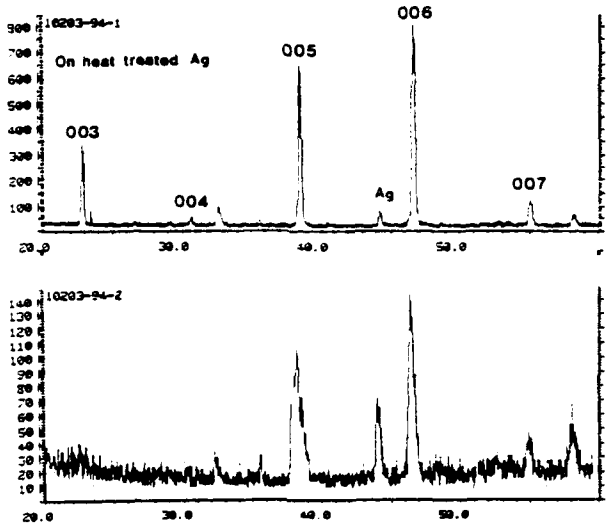

Fig. 14. C-axis oriented 123 film on silver substrate

TABLE II
SUMMARY OF THE PROPERTIES OF Y123 FILMS ON VARIOUS SUBSTRATES

	Mixed Ligand Solution			Metal Alkoxide and Copper Organic Salt Solution Copper (II) 2-Ethylhexanoate Process (2-EH)		
Substrate	YSZ	Ag	$SrTiO_3$ (100)	YSZ	Ag	$SrTiO_3$ (100)
Annealing	10 min at 921°C 24 hr at 405°C	1 min at 921°C 24 hr at 405°C	10 min at 903°C 31 hr at 400°C	10 min at 920°C 7 hr at 400°C	3 hr at 920°C 10 hr at 400°C	<1 min at 821°C 19 hr at 400°C
T_c	$T_{50.\rho}$ = 91 K δT_ρ = 4 K	$T_{50.\chi}$ = 63 K δT_χ = 50 K T_{ONSET} = 88-90 K χ_{fc}/χ_{zfc} = 0.5	$T_{50.\rho}$ = 86 K δT_ρ = 16 K	$T_{50.\rho}$ = 78 K δT_ρ = 20 K	$T_{50.\chi}$ = 63 K δT_χ = 50 K T_{ONSET} = 85-90 K χ_{fc}/χ_{zfc} = 0.5	$T_{50.\chi}$ = 77 K δT_χ = 12 K
Structure	Oriented: <30[a] Submicron Crystallites	Oriented: <20 Submicron Crystallites	Oriented: 50 0.5 to 2 Micron Crystallites		Oriented: 200 Flat <10 μm Crystallites	Oriented: 33 Fine Grains ~1 μm
J_c (0 g, 30 K)	300 A/cm^2					400 A/cm^2

[a]Orientation: (I_{006}/I_{103}) random oriented.

YBCO Coating on Complex Surface Geometry

Figure 15 shows that a smooth coating was obtained on both the inner and outer walls of a silver cylinder. The temperature dependence of the surface resistance of the coating on a 0.5 in. diameter silver disk, which corresponds tc a resonant frequency of 10.1 GHz, relative to an uncoated, polished silver disk of the same size was measured. As shown in Fig. 16, although the Q of the cavity with the coated disk improved dramatically as the temperature was decreased below 85 K, the coating was found to have a substantially higher surface resistance than Ag. The 123 coated Ag Q was 40,000 at 77 K and 62,000 at 29 K.

IV. SUMMARY AND CONCLUSION

The deposition of high temperature Y123 superconductor thin film on metal and ceramic substrates has been accomplished by dip coating using multimetal organic precursor compounds. Single phase pure $YBa_2Cu_3O_{7-x}$ thin film with transition temperature, T_c = 89 to 94 K was obtained at 900° to 920°C in oxygen for short time. C-axis alignment was obtained on Ag at 920°C for greater than 30 min. It is believed that the c-axis alignment was induced by a topotatic reaction with silver. Critical current density, J_c of the films were lower than anticipated due to the chemical reactions of the films with the substrates used. Diffusion barrier layer such as $BaZrO_3$ and or $LaACO_3$ should remedy the problem. A prototype high Q cavity was constructed and coated with Y123.

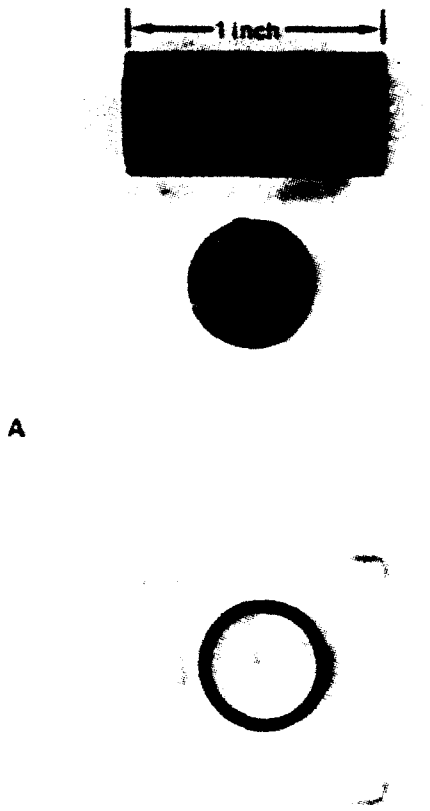

Fig. 15. Sol-gel derived 123 coated silver cylinder and caps (high Q cavity)

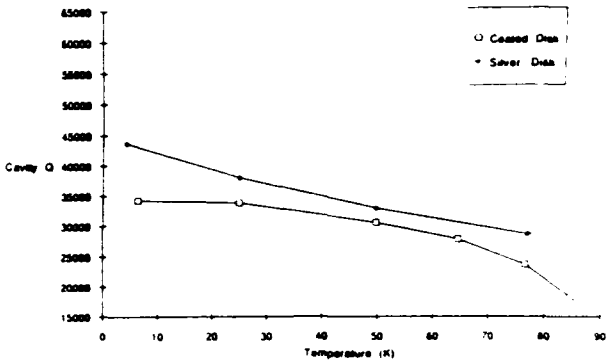

Fig. 16. Cavity Q and surface resistance measurement as a function of temperature

ACKNOWLEDGMENT

The authors wish to thank R. J. Precourt for his contribution in the design and construction of the "dipper," Salvacion Paguio for her assistance in preparation of metal organic precursor compounds. The work was supported by DARPA/ONR under Contract N00014-C-0714.

REFERENCES

1. M. K. Wu, J. R. Ashburn, C. J. Torng, P. H. Hor, R. L. Meng, L. Gao, Z. J. Huang, Y. Q. Wang, and C. W. Chu, "Superconductivity at 93 K in a New Mixed-Phase Y-Ba-Cu-O Compound System at Ambient Pressure," Phys. Rev. Lett. 58[9] 908-910 (1987).
2. Subramanian, J. S., et al., Science, 239, 1015-1017 (1988).
3. Sheng, Z. Z., et al., Phys. Rev. Letter, 60 10, 937-940 (1988).
4. R. W. Simon, C. E. Platt, A. E. Lee, G. S. Lee, K. P. Daly, M. S. Wire, J. A. Luine, and M. Urbanik, "Low-loss Substrate for Epitaxial Growth of High-Temperature Superconductor Thin Films," Appl. Phys. Lett., 53 [26] 2677-79 (1988).
5. B. Hammond, "Passive Microwave Devices and High-Tc Superconductors," Supercurrents, July, 1989, pp 66-71.
6. H. Dislich, "Thin Films from the Sol-Gel Process," in Sol-Gel Technology for Thin Films, Fibers, Preforms, Electronics, and Specialty Shapes, pp 50-79, L. Klein (ed.) Noyes Publications NJ, 1988.
7. H. Murakami, J. Nishino, S. Yaegashi, and Y. Shiohara, "Preparation of Y-Ba-Cu-O Superconductors by Sol-Gel Methods, ISTEC J., 3[2], 18-23 (1990).

8. A. R. Kaul, I. E. Korsakov, and A. V. Permjakov, "$YBa_2Cu_3O_{7-x}$ Thin Films: Some Problems of Synthesis and Ways to Solve Them," in Science and Technology of Thin Film Superconductors 2, pp 403-412, R. D. McConell and R. Noufi (eds), Plenum Press, New York, 1990.

9. R. H. Hammond, V. Jatijasevic, and R. Bormann, "Correlation Between In-situ Growth Conditions and Thermodynamic Stability Criteria for $YBa_2Cu_3O_y$, in Science and Technology of Thin Film Superconductors 2, pp 395-401, R. D. McConell and R. Noufi (eds.), Plenum Press, New York, 1990.

10. R. Bormann and J. Nolting, "Stability Limits of the Perovskite Structure in the Y-Ba-Cu-O System," Appl. Phys. Lett., 54 [21] 2148-2150.

11. S. Kramer, K. Wu, and G. Kordas, "Preparation of Thin Film $YBa_2Cu_3O_{6+x}$ Ceramic Superconductors by the Sol-Gel Process," Mat. Res. Soc. Proc., vol. 99, pp 323-6, Mat. Res. Soc., Pittsburgh, 1988.

12. S. Shibata, T. Kitagawa, H. Okazaki, T. Kimura, and T. Murakami, "Superconducting Oxides by the Sol-Gel Method Using Alkoxides," Jap. J. Appl. Phys., 27[1] L53-54 (1988).

13. S. Shibata, T. Kitagawa, H. Okazaki, and T. Kimura, "C-Axis-Oriented Superconducting Oxide Film by the Sol-Gel Method, Jpn. J. Appl. Phys., 27 [4] L646-48 (1988).

14. T. Manabe, H. Yokota, T. Kumagai, W. Kondo, and S. Mizuta, "Preparation of Superconducting $Ba_2YCU_3O_{7-\delta}$ Films by the Dipping-Pyrolysis Process using Metal Laurates," J. Ceram. Soc. Jpn. Inter. Ed., 98 [229-23e], 109-113 (1990).

15. P. Barboux, J. Taracson, L. Greene, G. Hull, and B. Bagley, "Bulk and Thick Films of the Superconducting Phase $YBa_2Cu_3O_{7-y}$ Made by Controlled Precipitation and Sol-Gel Processes," J. Appl. Phys., 63 [8] 2725-9 (1988).

16. C. E. Rice, R. B. van Dover, and G. J. Fisanick "Superconducting Thin Films of High Tc Cuprates Prepared by Spin-On/Pyrolysis," in Thin Film Processing and Characterization of High Temperature Superconductors, pp. 198-203, J. M. E. Harper, R. S. Colton, and L. C. Feldman (eds.), Am. Vac. Soc., New York, 1988.

17. T. Kumagai, W. Kondo, H. Yokota, H. Minamiue, and S. Mizuta, "Preparation of Superconducting $Ba_2YCu_3O_{7-\delta}$ Thin Films by the Dipping-Pyrolysis Process Using Metal Nephthenates and Acetylacetonates," J. Ceram. Soc. Jpn. Inter. Ed., 97 444-51 (1989).

18. C. E. Rice, R. B. van Dover, and G. J. Fisanick, "Preparation of Superconducting Thin Films of $Ba_2YCu_3O_7$ by a Novel Spin-On Pyrolysis Technique," Appl. Phys. Lett. 51 [22] 1842-44 (1987).

19. E. C. Behrman, et. al., "Synthesis, Characterization, and Fabrication of High Temperature Superconducting Oxides," Adv. Cer. Mat. 2[3B] 539-55 (1987).

20. T. Nonaka, K. Kaneko, T. Hasegawa, K. Kishio, Y. Takahashi, K. Kobayashi, K. Kitazawa, and K. Fueki, "Ba-Y-Cu-O Thin Films Fabricated by Dip Coating Using Concentrated Mixed Alkoxide Solution," Jpn. J. Appl. Phys., 27 [5] L867-69 (1988).

21. A. H. Hamdi, J. V. Mantese, A. L. Micheli, R. C. O. Laugal, D. F. Dungan, Z. H. Zhang, and K. R. Padmanabhan, "Formation of Thin Film High Tc Superconductors by Metalorganic Deposition," Appl. Phys. Lett. 51 [25] 2152-54 (1987).

22. S. Hirano, T. Hayashi, and M. Miura, "Preparation of $Ba_2YCu_3O_{7-\delta}$ Thin Films with Preferred Orientation through an Organometallic Route," J. Am. Ceram. Soc., 73 [4] 885-88 (1990).

23. C. Barbe and T. Ring, "Synthesis of Superconducting Thin Films by Organometallic Decomposition," in Better Ceramics Through Chemistry, IV, pp 883-887, B. J. J. Zelinski, C. J. Brinker, D. E. Clark, and D. R. Ulrich (eds.), Materials Research Society, Pittsburgh, Pennsylvania, 1990.

24. S. A. Kramer, G. Kordas, J. McMillan, G. C. Hilton, and D. J. Van Harligen, "Highly Oriented Superconducting Thin Films Derived from the Sol-Gel Process," Appl. Phys. Lett. 53 [2] 156-58 (1988).

25. T. Manabe, T. Kumagai, H. Minamiue, S. Nakamura, and S. Mizuta, "Reaction Between Films and YSZ Substrates during Preparation of $Ba_2YCuO_{7-\delta}$ Superconductor Films by the Dipping-Pyrolysis Process, J. Ceram. Soc., Japn. Inter. Ed., 98 82-87 (1990).

26. G. E. Whitwell, J. W. Wandas, F. M. Cambria, and M. F. Antezzo, "Solution-Derived $YBa_2Cu_3O_{7-\delta}$ Thin Films and Barrier Layers," in Better Ceramics Through Chemistry, IV, pp 929-934, B. J. J. Zelinski, C. J. Brinker, D. E. Clark, and D. R. Ulrich (eds), Materials Research Society, Pittsburgh, Pennsylvania, 1990.

27. G. A. Moore, D. Kenzer, M. Teppe, and G. Kordas, "Characterization of Amorphous Gel to Superconducting Oxide Conversion for Sol-Gel Produced $YBa2Cu3_{7-x}$" in Better Ceramics Through Chemistry, IV, pp 953-948, B. J. J. Zelinski, C. J. Brinker, D. E. Clark, and D. R. Ulrich (eds), Materials Research Society, Pittsburga, Pennsylvania, 1990.

28. C. T. Cheung and E. Ruckenstein, "Superconductor-Substrate Interactions of the Y-Ba-Cu Oxide," J. Mater. Res., 4[1] 1-15 (1989).

29. T. Hashimoto, K. Fueki, A. Kishi, T. Azumi, and H. Koinuma, Thermal Expansion Coefficients of High-Tc Superconductors," Jpn. J. Appl. Phys., 27[2] L214-L216 (1988).

30. K. S. Mazdiyasni, C. T. Lynch, and J. S. Smith, "The Preparation and Some Properties of Yttrium, Dysprosium, and Ytterbium Alkoxides," Inorg. Chem., 5[3] 342-46 (1966).

31. K. S. Mazdiyasni, "Chemical Synthesis of Single and Mixed Phase Oxide Ceramics," Mat. Res. Soc. Symp. Proc., vol 32, pp 175-86, Elsevier Science Publishing Company, Inc., New York, 1984.

32. K. S. Mazdiyasni, "Powder Synthesis form Metal-Organic Precursors," Ceramics International, 8[2] 42-56 (1982).

33. W. G. Fahrenholtz, D. M. Miller, and D. A. Payne, "Preparation of $YBa_2Cu_3O_{7-\delta}$ from Homogeneous Metal Alkoxide Solution," Ceramic Superconductors II, Man Yan (ed.), pp 141-147, Am. Cer. Soc. Westerville, Ohio, 1988.

34. Naito, M. et al., J. Material Research, 2[6], 713 (1987).

35. Cheung, C. T., and E. Ruckenstein, "Superconductor-Substrate Interactions of the Y-Ba-Cu Oxide," J. Materials Research, 4[1], 1-15 (1989).

END